

POLITECNICO DI TORINO

Master's Degree in ICT for Smart Societies



Master's Degree Thesis

From intracranial signals decoding to FES: a first approach using simulation of electrical pulses for objects grasping

Supervisors

Prof. Michela MEO

Prof. Robin AUGUSTINE

Dr. Mauricio PEREZ

Prof. Guido PAGANA

Candidate

Elena Roxana MAROLICARU

December 2022

Abstract

Nowadays, there is a growing interest in those people with a lack of limb movement ability, with the aim of giving them the capacity to perform voluntary movements, for instance, through supporting exoskeletons or through electrical muscle stimulation. In some cases, these are people who have undergone amputations of one or more limbs, in other cases they are patients with SCI. The MMG group at Uppsala University, which hosted the development of this project, aims to open the door to a new way of developing BCIs, as suggested by their work in B-CRATOS, an ambitious interdisciplinary project of which several partners are part. The present work falls within this context, with the objective of simulating the muscular stimulation through Functional Electrical Stimulation (FES) technique starting from decoding intracranial signals with Artificial Intelligence (AI). The methodology of this project starts from the processing of spiking activity and hand movement data collected from a macaque monkey while performing the task of grasping objects with different shapes and sizes. The data were collected by the German Primate Center in the context of the B-CRATOS project and made available for this work. Following in the methodology is the analysis of the muscles of the hand and arm involved in the grasping and release task of the objects used in the experiment and then the simulation of the FES signals with the definition of the electrical parameters (waveform, amplitude, frequency, pulse duration, relative delay of the specific muscle in relation to the other muscles). The last stage of the methodology is the search and choice of a proper architecture to decode intracranial input signals and give as output electrical stimulation parameters. After an in-depth literature search, eleven hand and arm muscles were selected, and simulations of the FES signals were performed. Then, electrical parameters to achieve the correct combinations of stimuli were generated for each type of grasping present in the dataset. The preliminary investigation of a suitable Neural Network architecture suggested using a decoder architecture mixing Convolutional Neural Network (CNN) and Long Short-Term Memory (LSTM) as in previous work in the MMG group. This work, based on the simulation of FES signals, seems to be optimistic in the context of muscle stimulation, which for those who still have undamaged limbs and muscles but not the capacity for voluntary movement is a viable option to be able to perform basic movements.

A Giulia, Emanuele, Felipe

Table of Contents

List of Tables	VI
List of Figures	VII
Acronyms	X
1 Introduction	1
1.1 Context	1
1.2 Objective	2
2 Background	4
2.1 Brain signals recording techniques	4
2.2 Muscle stimulation	7
2.3 Functional Electrical Stimulation	7
3 Dataset	10
3.1 Experiment description	10
3.2 Dataset format	11
3.3 Preliminary dataset filtering	12
4 Methodology	15
4.1 Muscle selection	15
4.2 FES signals	18
4.2.1 Waveform	19
4.2.2 Pulse amplitude	21
4.2.3 Pulse duration	22
4.2.4 Frequency	22
4.3 Dataset labels construction	22
4.4 Brain signals decoder	25
4.4.1 Decoders selection	26
4.4.2 Adaptation to new outputs	28

4.4.3	Hyperparameters optimization	30
4.4.4	Training, validation and test	31
5	Results	32
5.1	Muscle selection	32
5.2	FES signals	34
5.3	Dataset labels construction	34
5.4	Brain signals decoder	37
5.4.1	Hyperparameters optimization	37
5.4.2	Training, validation and test	39
6	Conclusions	45
6.1	Future work	45
	Bibliography	47

List of Tables

2.1	EEG frequency bands. [15]	5
2.2	Brain signals recording techniques comparison.	6
3.1	Objects and corresponding original labels in the dataset.	14
5.1	Chosen muscles and their codification for the software development.	33
5.2	Set of parameters.	35
5.3	Muscle stimulation configurations.	36
5.4	Occurrences of labels in the original and in the filtered datasets.	37
5.5	Optimum hyperparameters.	39
5.6	Accuracy for different values of dropout fraction.	44

List of Figures

2.1	10-20 international system of electrode placement.	5
2.2	Skeletal muscle composition[22].	7
2.3	FES stimulation.	8
3.1	Arrays implantation. [10].	11
3.2	Experiment setup. [10].	12
3.3	Dataset structure.	13
3.4	Preliminary filtered dataset.	14
4.1	Thenar muscles group [27].	16
4.2	Flexor digitorum superficialis muscle [28].	16
4.3	Extensor digitorum communis muscle [29].	17
4.4	Adductor pollicis muscle. [27].	18
4.5	Hypothenar muscles. [27].	18
4.6	Dorsal and palmar interossei. [27].	19
4.7	Lumbrical muscles. [27].	19
4.8	Wrist movements.	20
4.9	FES stimulator parameters [25].	20
4.10	Waveforms for FES [25].	21
4.11	Labels creation - first step. [40].	23
4.12	Two phases grasping movement.	24
4.13	Labels creation - second step. [40].	24
4.14	Grasping type example for small objects.	25
4.15	Labels creation - thrid step.	25
4.16	Example of original label and corresponding new label.	26
4.17	Dense Neural Networks.	27
4.18	Recurrent Neural Network vs Feed Forward Neural Network [42].	28
4.19	LSTM Neural Network structure [44].	29
5.1	Stimulation signals.	35
5.2	Configurations and corresponding objects.	36

5.3	Dense Neural Network loss evolution.	40
5.4	Simple Recurrent Neural Network loss evolution.	40
5.5	LSTM Neural Network loss evolution.	41
5.6	Ensemble Neural Network loss evolution.	41
5.7	Accuracy with optimized hyperparameters for DNN and RNN. . . .	42
5.8	Ensemble accuracy.	43
5.9	LSTM accuracy.	44

Acronyms

AI

Artificial Intelligence

BCI

Brain Computer Interface

B-CRATOS

Brain-Connect interRfAce TO machineS

ECG

Electrocardiography

EMG

Electromyography

EOG

Electrooculography

FES

Functional Electrical Stimulation

fMRI

functional Magnetic Resonance Imaging

fNIRS

functional Near-Infrared Spectroscopy

NMES

Neuromuscular Electrical Stimulation

SCI

Spinal cord injury

SNR

Signal-To-Noise Ratio

TPE

Tree Parzen Estimator

Chapter 1

Introduction

1.1 Context

Complications in voluntary movement and even severe paralysis can result from various pathological or traumatic conditions. The damage can be at the level of the brain, the spinal cord, peripheral nerves or at the level of the muscles [1]. To give an example, there are between 250,000 and 500,000 people suffering from SCI every year in the world [2]. In 2017 there were 57.7 million people with limb amputation worldwide [3]. In most cases, the damage that leads to a motor deficit is due to traumatic events, such as car accidents, and it is estimated that cases will increase in the coming years. The development of motor neuroprostheses fits into this context as a means of trying to restore the ability of voluntary movements to this class of patients. The aim of the neuroprostheses is not just to aesthetically recreate the shape of the missing limb, but to restore the functionality of the limb itself [4, 5].

Over the last decade, several projects have been initiated with the aim of developing neuroprostheses: NeuraViPeR, which focuses on visual neuroprostheses [6], MoreGrasp project, which focuses on grasping using non-invasive EEG signals [7], BCINET, which focuses on developing BCIs to make them more suitable for neuroprosthetic applications [8], B-CRATOS, which aims at the construction of a brain-controlled, wireless prosthetic arm [9].

The B-CRATOS (Brain-Connect interRfAce TO machineS) project, in particular, which wants to expand the boundaries of neuroprostheses, aims at the development of a bidirectional intra-body battery-free wireless brain-machine-body communication, which decodes brain signals and transforms them into signals for a biomechatronic prosthetic upper limb. The B-CRATOS project's partners are Uppsala University, SINANO Institute, Scuola Superiore Sant'Anna, Blackrock Microsystems Europe GmbH, LINKS FOUNDATION, Deutsches Primatenzentrum

GmbH, Norwegian University of Science and Technology (NTNU).

The thesis project was developed at the MMG group, Uppsala University, in the context of the B-CRATOS project, and is based on the previous work of Federico Fabiani, a master student from Politecnico di Torino who also carried out his thesis project at the MMG group. His work focused on the implementation of different types of decoders with the aim of actuating a biomechanical arm. In particular, Fabiani developed different types of decoders for decoding neural signals in his project and implemented the best of them in real time for the actuation of the mechanical arm.

However, there are cases in which the limbs are intact and the nerves are not completely damaged. In this case, an alternative approach to biomechanical prosthetics may be direct stimulation of the muscles using electrodes.

In the present work, the type of neuroprosthesis considered is the one that uses functional electrical stimulation (FES), a technique used to stimulate specific muscles with the aim of performing a specific function, in this case grasping objects. This type of neuroprosthesis requires that the motor neuron is undamaged.

The field of neuroprosthetics is full of difficulties to overcome, starting with the recording of brain signals. Neural recording techniques are diverse, some invasive and others non-invasive, and, in the choice, one must always make a trade-off between different requirements (cost, signal noise, invasiveness, etc.). Moreover, the stimulation of muscles, as mentioned, requires their structure and innervation to be intact. If these requirements are not met, the FES technique is not applicable. In such cases, it may be convenient to use mechanical prostheses.

1.2 Objective

The main objective of this thesis project is to develop a first approach for muscle stimulation using the Functional Electrical Stimulation technique from the decoding of intracranial signals from a macaque monkey. The FES technique is used in neuroprosthetics to restore muscle movement. The FES treatment consists of applying an external current to stimulate the muscle and thus its movement. In this work, in particular, the goal is not the stimulation of a single muscle, but of a group of muscles in the hand and arm to enable the action of grasping different types of objects. The way to achieve this goal involves the development of several steps.

1. The first step is the study of the dataset containing data on the neural activity captured by the motor cortex of a macaque monkey during the grasping task [10], and the study of the analysis work carried out on this dataset in a previous work at the MMG group [11]. It is expected to eliminate certain elements of the dataset according to what is needed for the purposes of this

project.

Output of the step: preliminary filtration of the dataset.

2. Secondly, a study of the literature must be carried out on the muscles involved in the action of grasping objects and select a limited number of them to compose an elementary group of muscles involved in the grasping action.
Output of the step: the group of muscles that are supposed to be stimulated to achieve certain types of grasping.
3. A literature search must be carried out on FES signals to understand their general characteristics and the electrical parameters involved in the stimulation of the muscles and then simulating them according to the stimulation purpose.
Output of the step: set of parameters to be programmed for the FES technique and the values decided for these parameters.
4. After completing the previous objectives, there is the step of constructing new labels for the dataset. At this stage, the goal is to have a dataset containing the intracranial neural signals of the macaque monkey and a label type for each task that is suitable for the final goal of using the FES technique. We will no longer have the object types as labels for each task, but a description of the muscles to be stimulated and the way to do it.
Output of the step: new labels, consisting of as many entries as there are muscles and each corresponding to a set of stimulation parameters.
5. The last phase of the work is the adaptation to the purpose of stimulation with the FES technique of different types of decoders previously developed at the MMG group that had as their objective the actuation of a mechanical arm.
Output of the step: choice of decoders, their adaptation to new labels and offline testing.

Chapter 2

Background

2.1 Brain signals recording techniques

Recording techniques used for BCIs and neuroprosthetics are classified in non-invasive and invasive. In Tab.2.2 the main differences between the techniques presented in this section can be observed.

- Electroencephalography (EEG) is the most popular non-invasive method when it comes to BCIs and neuroprosthetics. Indeed, EEG is an inexpensive technique, the device is very portable, and does not require surgery to implant the electrodes. In EEG, electrodes are placed directly on the scalp with the international 10-20 system, as shown in Fig.2.1. The electrodes placed on the scalp are sensitive to voltage potentials from current flows between neurons. The end result obtainable with the EEG is not the recording of action potentials, but of electrical activity in large portions of the brain [12]. The signals obtained are classified according to their frequency, amplitude, and the area from which they were recorded. This variety of characteristics is informative of the type of action performed and the area from which the signal originates. A classification of EEG signals by frequency is observed in Tab.2.1. A strong limitation of EEG signals is contamination by artifacts due to ECG, EMG, EOG signals, which have large amplitudes at low frequencies, and power-line noise [13]. However, part of these disturbances is removed in the preprocessing phase of BCIs. In addition, EEG does not enjoy good spatial resolution, which is on the order of centimeters. Nevertheless, EEG remains an attractive technique for real-time BCIs and neuroprosthetics because of its high temporal resolution of the order of milliseconds [14].

- Functional Near-Infrared Spectroscopy (fNIRS) is a non-invasive optical technology that monitors the hemodynamic response in the cerebral cortex. It has local measurements of oxy-hemoglobin (O₂Hb) and deoxy-hemoglobin (HHb) concentration changes in cortical areas of the brain. Within this technique, one works with optodes (emitters and detectors) and uses at least 2 wavelengths in the near-infrared spectrum. The penetration capacity of the near-infrared light through tissue and bone is 2-3 cm. It is a technique that is becoming increasingly popular in the world of BCIs because of the high portability and limited cost. However, the temporal resolution is on the order of hundreds of ms, as with fMRI, while the spatial resolution is even worse for physiological response [17].
- Intracranial electroencephalography (iEEG) is an invasive brain signal recording technique. It is performed using intracranial electrodes. It is called ECoG (Electrocorticography) when using grids of electrodes implanted in the subdural space. The temporal resolution that is achieved with EEG is in the order of ms, since a sampling rate of 1000-3000 Hz is used. The temporal resolution is therefore similar to that of EEG. What you have more in compared to EEG is the spatial resolution (order of mm) since you have a high localization of the signal origin, and the signal to noise ratio (SNR). In fact, many of the sources of noise such as tissue thickness, cardiac and respiratory artifacts, and electromagnetic noise disappear as you get closer to the signal source of interest. In addition, used during experiments it allows you to avoid the overtraining that is necessary when you have a lot of noise to handle [18].

Technique	Type	Temporal resolution	Spatial resolution
EEG	non-invasive	~ ms	~ cm
fMRI	non-invasive	100 ms	~ mm
fNIRS	non-invasive	100 ms	1 cm
iEEG	invasive	~ ms	~ mm

Table 2.2: Brain signals recording techniques comparison.

As can be seen in the summary table 2.2, the best performances in terms of temporal and spatial resolution can be obtained with iEEG, which, unlike the others proposed, is an invasive recording technique. The experiment that originated the dataset used in this thesis is based on the recording of brain signals using iEEG.

2.2 Muscle stimulation

The muscles type of interest in this thesis project is the skeletal muscle (Fig.2.2), which consists of elongated muscle fibres, whose cytoplasm contains bundles of myofibrils that have the function of making the muscle contract and relax. The basic unit of the myofibril is the sarcomere. Contraction of the sarcomeres leads to macrocontraction of the muscle. Each sarcomere is composed of thick filaments (consisting of myosin) and thin filaments (consisting of actin). The sliding of the thin filaments over the thick ones is what we call muscle contraction [19]. Several muscle fibres are innervated by the same motor neuron (motor unit). The number of motor units influences the strength of the contraction. The contraction of the muscle fibres occurs through neural control, thanks to action potentials triggered by the summation of electrical potentials on the postsynaptic membranes, and transmitted through excitable cells [20] that depolarise the muscle cell membranes. This effect can also be achieved by external stimulation, by transmitting trains of electric pulses to muscles and nerves [21].

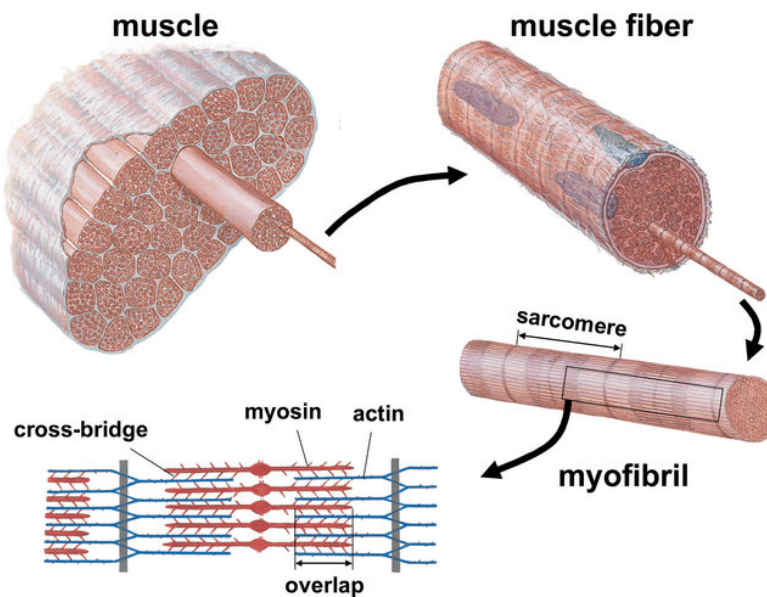


Figure 2.2: Skeletal muscle composition[22].

2.3 Functional Electrical Stimulation

Functional Electrical Stimulation (FES) is a muscle stimulation technique based on the use of low-energy electrical pulses that interact with nerves and muscles to

generate movement or sensation [23] (Fig.2.3). It is a technique that originated in

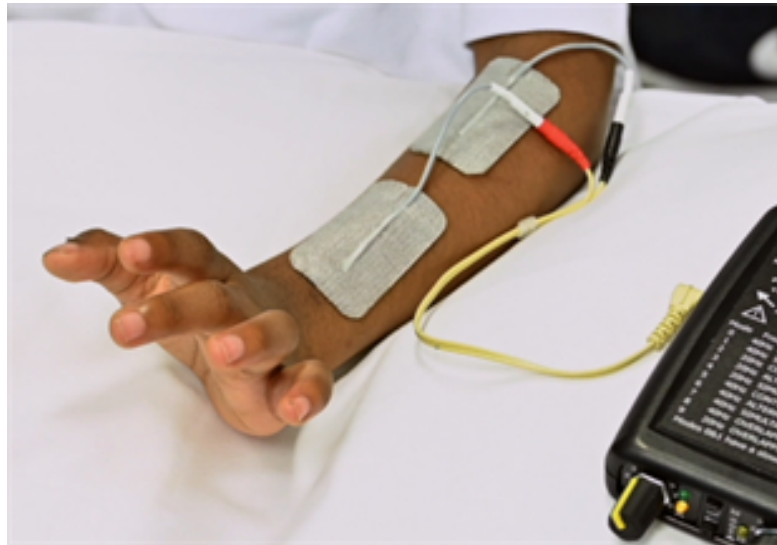


Figure 2.3: FES stimulation.

the 1960s and since then its potential has developed in various fields of application. In rehabilitation, the FES technique is a potentially good solution to paralysis, its ambition being to restore the possibility of voluntary movement to people with paralysis. FES is a subcategory of NMES (NeuroMuscular Electrical Stimulation) techniques. NMES consists of applying an electric current to produce muscle contraction. The way NMES works is based on the forcing of membrane depolarisation: when an electric current is supplied to the tissue, an electric field is generated in the vicinity of the motor axons that is able to depolarise the membranes of the axons. This leads to the generation of action potentials that propagate leading to muscle contraction. Since the technique is based on the depolarisation of the motor axons, the peripheral nerves must be intact for the stimulation to work. Therefore, the applications of this technique are limited to subjects who do not have muscle weakness or peripheral nerve damage, i.e. patients with SCI, traumatic brain injuries, multiple sclerosis or stroke patients [24]. FES is a type of NMES in which stimulation is aimed not at contracting and reducing muscle damage, but at functional movements, such as grasping objects [25]. This makes the FES technique a very valuable tool in the design of motor neuroprostheses.

The fundamental elements of an FES-based neuroprosthesis are the stimulator, the electrodes through which stimulation pulses are transmitted to the tissues, and the sensors for controlling the stimulation, which can be voluntary or automatic [25]. The stimulator is the part of the system where the stimulation parameters are defined (waveform, current amplitude, frequency and duration of stimulation) and

can be characterised by several channels, consisting of pairs of anode and cathode, each dedicated to the stimulation of a muscle.

Stimulation electrodes can be either invasive (implanted or percutaneous electrodes) or non-invasive (transcutaneous electrodes). The main advantages of non-invasive electrodes are the absence of surgery and the possibility of changing the position of the electrodes, making this type of electrodes a rather flexible solution. With implanted or percutaneous electrodes, on the other hand, the position of the electrodes is definitive following surgery and there is no possibility of calibration in the event of incorrect position for stimulation. On the other hand, transcutaneous electrodes require higher currents in order to reach the tissue, with values of up to 120mA, whereas invasive electrodes require currents around 25mA [25].

Chapter 3

Dataset

The dataset used for this thesis was produced by researchers at the German Primate Center and Department of Biology, University of Göttingen, following an experiment conducted on two macaque monkeys (animal Z, female, and animal M, male). The experiment is described in "Decoding a Wide Range of Hand Configurations from Macaque Motor, Premotor, and Parietal Cortices" [10] and a summary is presented in this section.

3.1 Experiment description

After being trained to grasp different objects while wearing a kinematic data glove, electrode arrays were implanted in the cortical areas AIP, F5 and M1, as shown in Fig.3.1. A total of 192 electrodes were implanted. With these, while the macaque monkeys performed the tasks, spiking activity was recorded using a sampling rate of 24kHz. The experiment can be described through several epochs, also shown in Fig.3.2c for object grasping and Fig.3.2e for precision and power grips. The main epochs are listed below.

- Fixation epoch: the monkey sitting in the dark on a chair in front of a turntable containing objects in a pseudo-random order 25cm from the chest level, presses a button near the chest. While continuing to keep his hand on the button, he must continue to stare at a red LED light. The average duration of this epoch is 650 ms.
- Cue epoch: a light is switched on to illuminate the object. The monkey continues to stare at the object during this epoch. Its duration is 700 ms.
- Planning epoch: The monkey continues to stare at the object without moving until the red LED light flashes. The average duration of this epoch is 800 ms.

- Movement epoch: The LED light blinks giving the signal to the monkey to move to grasp the object.
- Hold epoch: the monkey must hold the object for 500 ms, after which it is given juice.

After a inter-trial duration of 1000ms, a new trial begins.

There are 8 turntables used in the experiment, with 6 objects on each turntable. When each object has been grasped on the turntable, the next turntable is presented to the monkey until all turntables are shown. In addition to grasping objects, power and precision grips were also performed on a handle. Specifically, after grasping all objects on all turntables, 10 trials were performed on precision and power grips. The whole setup of the experiment can be seen in Fig.3.2.

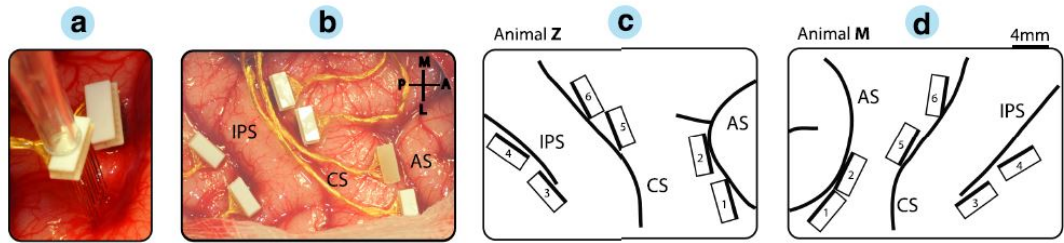


Figure 3.1: Arrays implantation. [10].

3.2 Dataset format

The data used in this project are those recorded by the male monkey. Of the original 759 trials, only 628 were correct, while the remained ones were eliminated due to monkey errors during the experiment. These data were pre-processed with spike sorting algorithms, resulting in 552 isolated firing neurons. In the original format, each neuron unit was represented by a series of timestamps, corresponding to the instants at which the neuron fired, but the dataset was then reshaped to have a structure more suitable to become an input for the neural network. The final form of the dataset provides for each trial a matrix in which the rows correspond to the neurons and the columns correspond to the time bins into which the total time of the trials was divided. In each cell is the number of times the neuron fired in that time bin. The label of each matrix is the object grasped during the corresponding trial. The duration of each time bin was set at 40 ms in the previous work[11], following the suggestion from researchers from German Primate Center and the average duration of an entire trial is 5.57 s. The total number of time bins per trial and thus columns in the corresponding matrix is 139. In Fig.3.3, a scheme

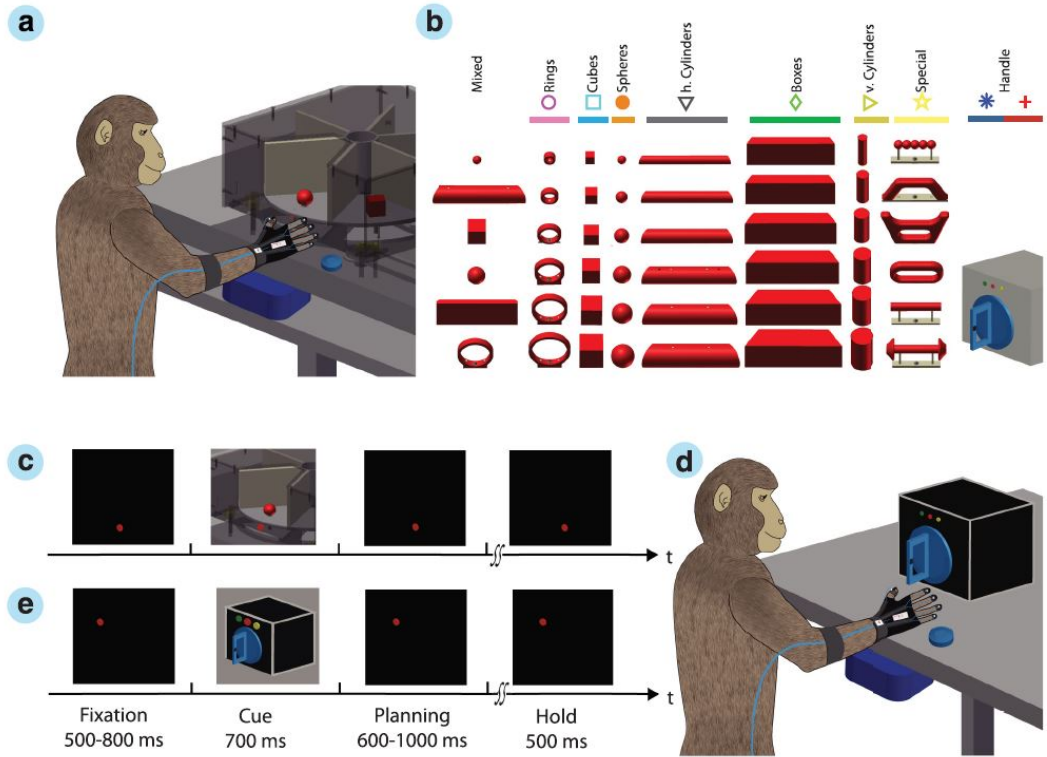


Figure 3.2: Experiment setup. [10].

of the structure of the dataset is shown.

3.3 Preliminary dataset filtering

Of the dataset containing only correct trials, which were therefore not eliminated due to monkey error, not all trials are actually considered. In fact, trials labelled with the object type 'special2' are eliminated, as the association of the objects with these trials is unclear. In addition, it was decided not to use the trials corresponding to grip precision and power, and to keep only the trials corresponding to the objects listed below.

- Ring, six sizes.
- Cube, six sizes.
- Ball, six sizes.

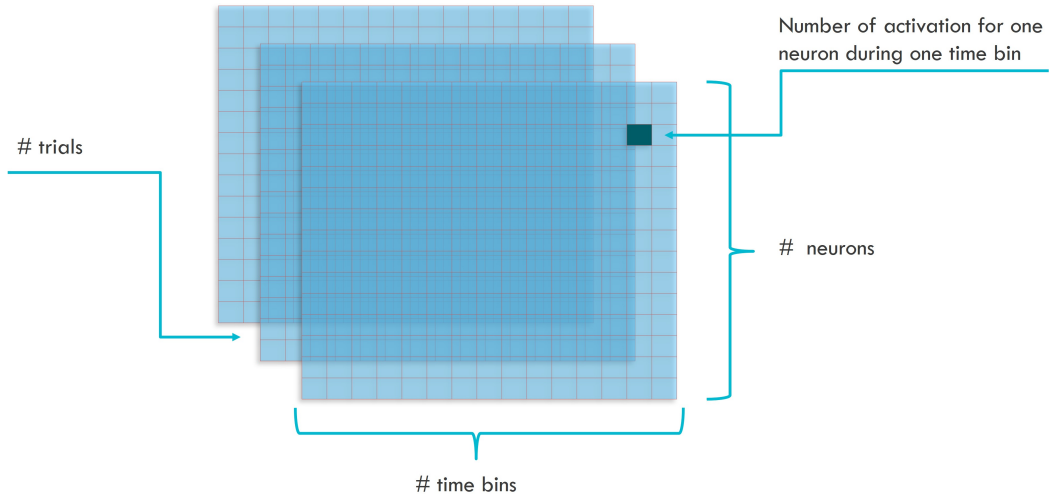


Figure 3.3: Dataset structure.

- Horizontal cilinder, six sizes.
- Box, six sizes.
- Vertical cilinder, six sizes.
- Special shapes.
- Mixed shapes, from the ones before.

In total, there are 46 different possible objects in the filtered dataset, if we exclude the objects belonging to the 'Mixed' group. Tab.3.1 presents the numeric codes associated with each object in the dataset. Each object is identified by a two-digit number: the first digit indicates the shape of the object and the second identifies the size, where "1" corresponds to the smallest size and "6" corresponds to the largest size. In the case of the horizontal cylinder, we have 8 different labels in the dataset, which might suggest that there are 8 different sizes. In reality, this is due to the fact that labels "57" and "58" relate to two different ways of grasping the cylinder with the largest size, identified by label "56". In addition to the filtering of tasks, a cut was also made on the duration of the trial then actually used in this work. In fact, since different hand conformations are to be realised, starting with the intention to grasp objects, it was decided to use only the data preceding the epoch "Hold" for prediction purposes. Thus, the dataset filtered so far actually consists of 472 trials, each containing the number of activations for 552 neurons in 74 time bins (Fig.3.4).

Object type	Sizes
Mixed	"11" "12" "13" "14" "15" "16"
Rings	"21" "22" "23" "24" "25" "26"
Cubes	"31" "32" "33" "34" "35" "36"
Balls	"41" "42" "43" "44" "45" "46"
hCylinder	"51" "52" "53" "54" "55" "56 57 58"
Boxes	"61" "62" "63" "64" "65" "66"
special	"71" "72" "73" "74" "75" "76 77 78"

Table 3.1: Objects and corresponding original labels in the dataset.

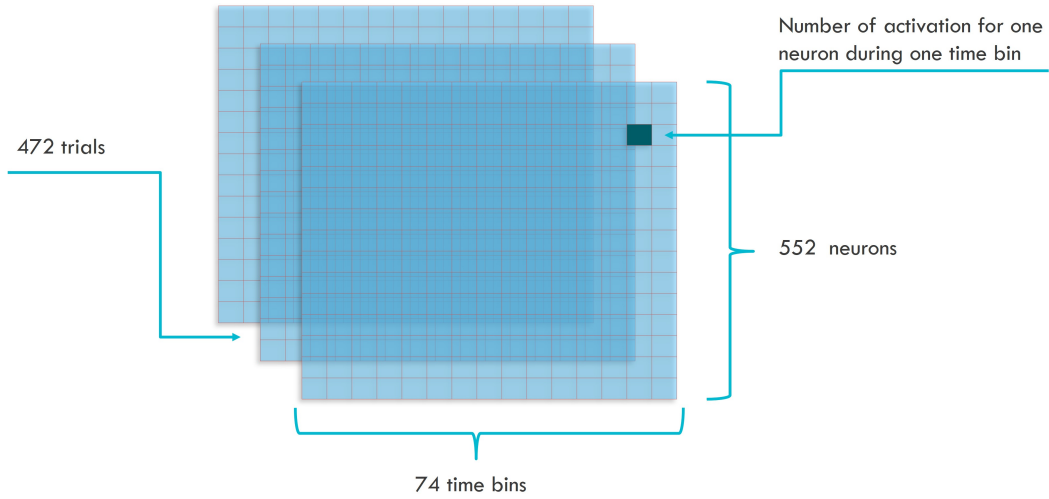


Figure 3.4: Preliminary filtered dataset.

Chapter 4

Methodology

4.1 Muscle selection

The operation of muscle selection was guided in its entirety by the experiment described in [10] that originated the dataset used in this thesis. In this experiment, the monkey had to grasp objects of different shapes and sizes (Fig.3.2b). By examining each object, a hypothesis was made of the type of grasping used to grasp each object. Subsequently, a literature study was carried out to identify the muscles of the hand and arm whose contraction and relaxation enable the grasping action of the objects described in the experiment.

A study that considered the action of grasping a macaque monkey of objects emphasises that during the grasping action, coordinated activation of the distal muscles is required [26]. They investigated the EMG recordings of different muscles during grasping. Each object was represented with a vector of muscles in order to characterise it from the point of view of muscle activity. In the study, some objects are similar in shape to the objects considered in the dataset used for this thesis: small and large cylinder, large disc, small and large plates, large sphere. In the grasping of these objects, the muscles that presented activation in the different phases of the movement are mainly the thenar muscles (Fig.4.1), active during grasping and when releasing the object, the flexor digitorum superficialis (Fig.4.2) and extensor digitorum communis muscles, both active in the first grasping phase. In particular, the thenar muscle is a muscle group comprising three muscles: the abductor pollicis brevis, the flexor pollicis brevis and the opponens pollicis. The abductor pollicis brevis is the muscle that makes the thumb move away from the index finger. The flexor pollicis brevis is the muscle that allows the thumb and little finger to move closer together. The opponens pollicis is the muscle that allows the thumb to move away from the other fingers, so as to allow the action of grasping objects. It is therefore one of the most important muscles when it comes

to grasping. In addition to the muscles highlighted in the study described above,

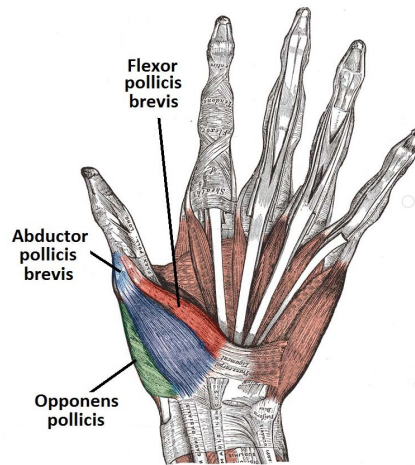


Figure 4.1: Thenar muscles group [27].

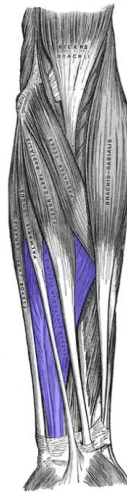


Figure 4.2: Flexor digitorum superficialis muscle [28].

other muscles of the hand have been identified that have a central function during grasping [30]. The adductor pollicis muscle (Fig.4.4), a muscle outside the thenar group, has the function of adducting the thumb.

The hypothenar is a group of three muscles involved in the movement of the little finger (Fig.4.5).

An important muscles group are the interossei, which consist of four dorsals and three palmar muscles (Fig.4.6): the dorsal interossei have the function of the

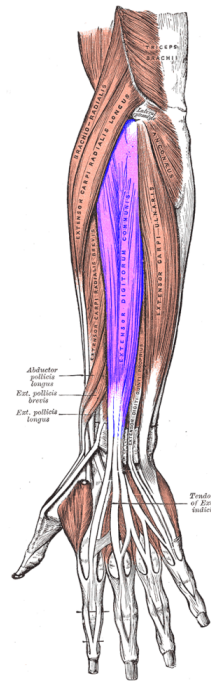


Figure 4.3: Extensor digitorum communis muscle [29].

abduction of the second, third and fourth digits, while the palmar muscles have the function of the adduction of the same.

The lumbrical muscles (Fig.4.7) are a group of four muscles that have the function of flexion of the metacarpophalangeal joint and extension of the proximal interphalangeal (PIP) and distal interphalangeal (DIP) joints.

The muscles described so far are extrinsic muscles, located superficially and therefore also suitable for stimulation. In addition to these, there are the intrinsic muscles are smaller muscles located more deeply, such as in the joints between the phalanges.

The flexor digitorum superficialis and extensor digitorum communis muscles, on the other hand, are muscles located in the arm. The flexor digitorum superficialis is the largest of the flexors in the forearm [31]. Its tendon inserts into all fingers and its function is to be the primary flexor of the proximal interphalangeal joints of the middle phalanges [32]. The extensor digitorum communis is another muscle located in the forearm that has the function of contributing to the extension of the wrist and digits two, three, four and five.

In the grasping movement, it is often necessary to also perform a rotation of the wrist, in particular to grasp vertically extended objects, such as the cylinders in Fig.3.2. Therefore, a study of wrist movements was also carried out. In particular,

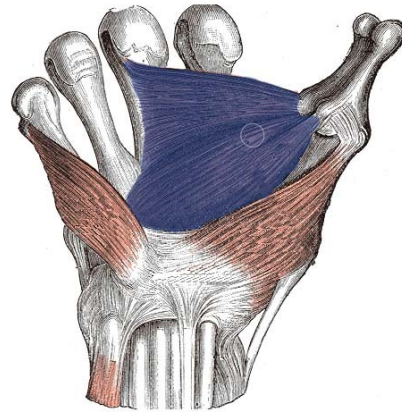


Figure 4.4: Adductor pollicis muscle. [27].

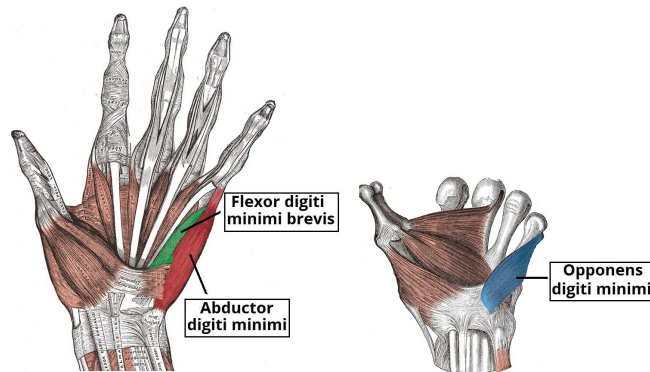


Figure 4.5: Hypothenar muscles. [27].

the circular movement of the wrist is given by the composition of several movements: flexion, extension, abduction and adduction of the hand (Fig.4.8). These movements are performed by different muscles: flexor carpi radialis and flexor carpi ulnaris [33], extensor carpi radialis and ulnaris [34], flexor digitorum superficialis [32], flexor pollicis longus [35], extensor digitorum longus [36] and extensor pollicis longus [37].

4.2 FES signals

At this stage of the methodology, the goal is to set the parameters of the stimulator, the part of the FES system responsible for generating the stimuli to be transferred

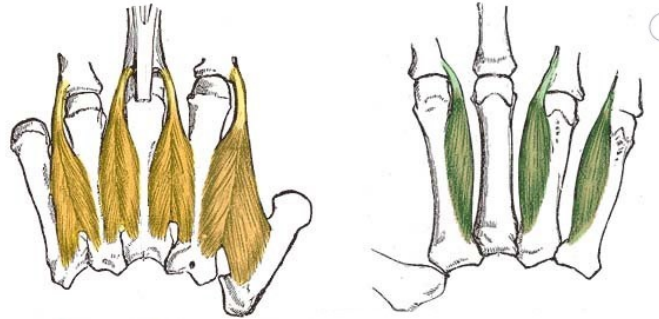


Figure 4.6: Dorsal and palmar interossei. [27].

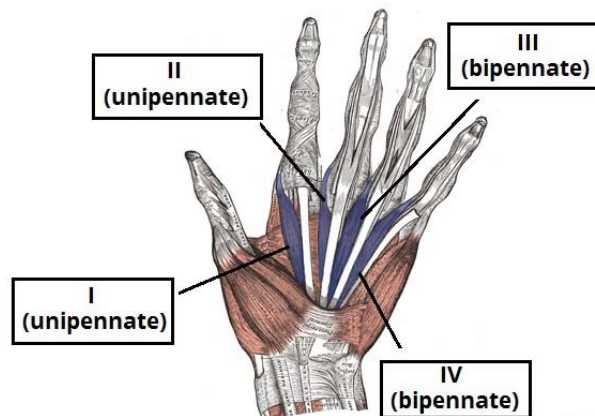


Figure 4.7: Lumbrical muscles. [27].

to the muscles in charge of performing the desired movements. In Fig.4.9 the parameters to be defined for the stimulation signal are shown.

4.2.1 Waveform

Since direct current is not suitable for this type of application and its effect is the production of a potential action in the moment and not a stimulation over time that allows movement, there is a need to look to alternating current waveforms for this type of stimulation [21]. Then, the main types of waveforms for FES applications

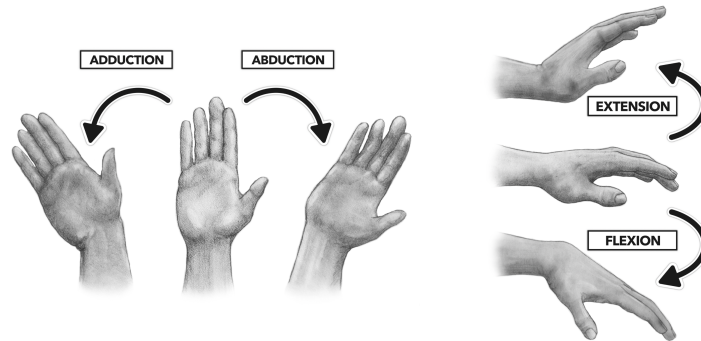


Figure 4.8: Wrist movements.

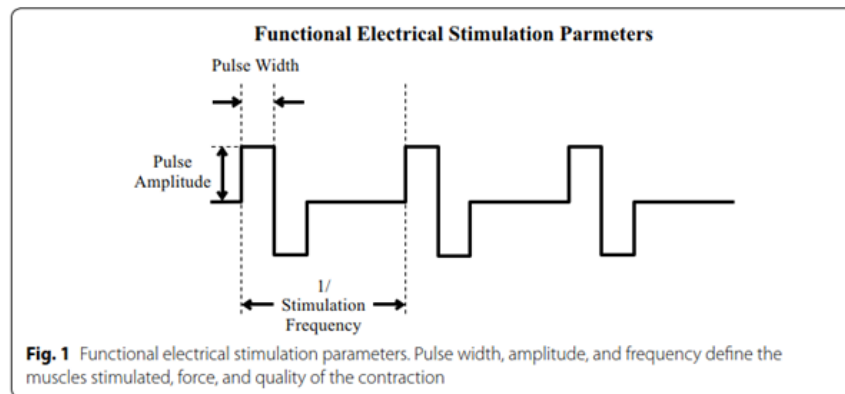


Figure 4.9: FES stimulator parameters [25].

are shown in Fig.4.10.

- Monophasic waveform is not recommended as it leads to a build-up of current in the tissue, whereas the optimum would be to have a zero balance between incoming and outgoing current [21].
- Biphasic waveforms are waveforms that ensure that the current transferred to the tissue is then removed.
 - Biphasic balanced waveforms generate a contraction under both the anode and the cathode. Usually, the first phase occurs under the cathode, while the second takes place under the anode. The latter aims to reverse the electrochemical process due to the first phase. Time is usually left between

the biphasic stimulations for the action potential to propagate correctly [23].

- Asymmetric balanced biphasic waveforms ensure that contraction occurs only under the cathode [23].

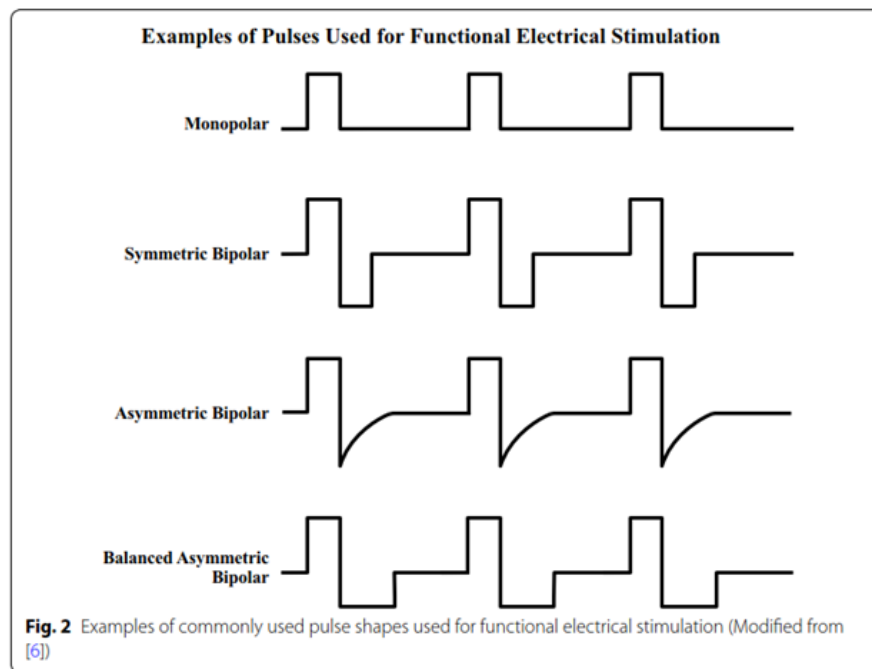


Figure 4.10: Waveforms for FES [25].

4.2.2 Pulse amplitude

Current intensity is what influences membrane depolarisation in stimulation. A higher intensity results in a higher depolarisation. In the parameters setting of the stimulator, the current intensity corresponds to the pulse amplitude (Fig.4.9). The current level depends on the particular muscle (size and properties). For applications similar to the one considered in this thesis, which is the stimulation of hand and arm muscles, typical current levels are 10-20 mA [21]. The choice of amplitude affects the type of nerve fibres recruited [25]. When choosing the stimulation current, attention must be paid to the effect of muscle fatigue. In fact, excessive current levels can either lead to no contraction effect in addition to that already achieved, or to muscle fatigue, thus decreasing the maximum contraction achievable [38].

4.2.3 Pulse duration

The pulse duration is the parameter identifying the time interval over the entire stimulation period for which the current intensity is on (Fig.4.9). The duration can be different depending on the targets: a high selectivity in muscle nerves is given by a very small pulse duration of the order of $10\mu\text{s}$ [39] and a very high current amplitude, while larger amplitudes result in stronger contractions with a lower current. Therefore, typically the pulse duration chosen in the FES environment is between $200\mu\text{s}$ and $500\mu\text{s}$ [21].

4.2.4 Frequency

Frequency is a parameter that influences the intensity of the transmitted signal: the higher the frequency, the higher the number of action potentials transmitted in the unit of time. Since FES is synchronous stimulation, unlike the physiological way of propagating action potentials, which results from the asynchronous recruitment of motor units to avoid fatigue, a higher frequency than the physiological one must be used. Typical values for obtaining upper limb movement range from 20 to 50 Hz. Above these values, there is less discomfort in the patient, but also faster achievement of muscle fatigue [21].

4.3 Dataset labels construction

After having defined the muscles to be stimulated and the signals through which to stimulate them, the following step was the construction of new labels in the dataset.

The original labels consisted of two-digit numbers identifying objects of different shapes and sizes. The aim is to change the two-digit number to a vector containing as many elements as muscles to be stimulated. Each element of the vector will consist of an integer value representing a set of electrical parameters with which the muscle has to be stimulated.

To achieve this, this phase of the methodology consists of several steps:

1. Each object in Fig.3.2a has been associated with an assumed movement to achieve grasping, as shown in Fig.4.11.

Depending on the shape and size of the object, the grasping dynamic changes. For example, in most cases, two successive movements are required for larger objects: starting with the relaxed hand, the first movement is the opening of the hand or specific fingers, so there is an abduction of the muscles; the second movement is the closing of the fingers to grasp the object in the hand, which is performed by adduction of the muscles (Fig.4.12). Therefore in these

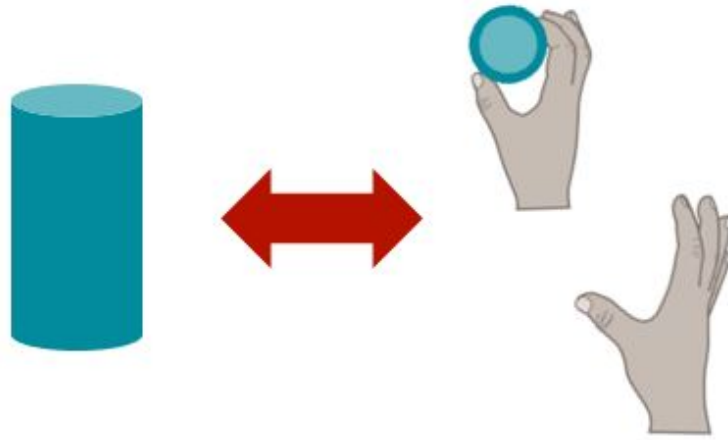


Figure 4.11: Labels creation - first step. [40].

cases the abduction muscles are activated before the adduction muscles. For smaller objects, on the contrary, it has been hypothesised to achieve grasping with only the flexion movement starting from the relaxed hand. In addition to the diversity of movement due to the diversity of sizes, there is variation due to the diversity of shape. A significant example of this is the large vertical cylinder, to grasp which requires first a twisting movement of the wrist combined with an opening movement of the fingers and then a bending movement. Grasping in this case requires the hand to be rotated approximately 90 degrees from the horizontal.

2. Once the dynamics of the different grasping types were understood, the muscles to be stimulated in the different phases of the movement or in the only phase and the muscles that do not need stimulation were defined within the chosen group of muscles (Fig.4.13).

For smaller objects, since it is not necessary to involve all the fingers in the movement (Fig.4.14), it can be assumed that only the thumb, index and middle finger can be used.

3. After defining the muscles to be activated in the two phases, one type of stimulation was associated to each muscle (Fig.4.15). Taking into account that for different objects the movement dynamics may be the same, it can be figured out a finite number of possible configurations.

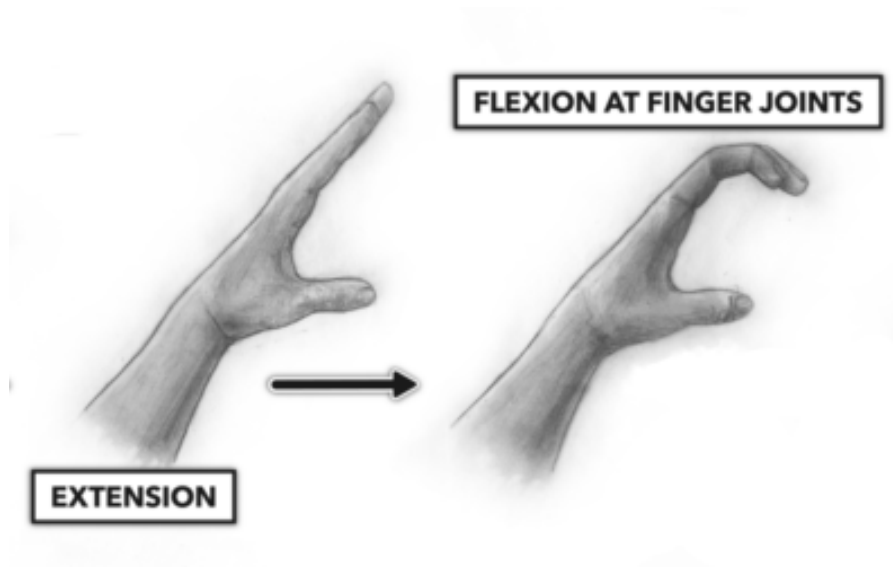


Figure 4.12: Two phases grasping movement.

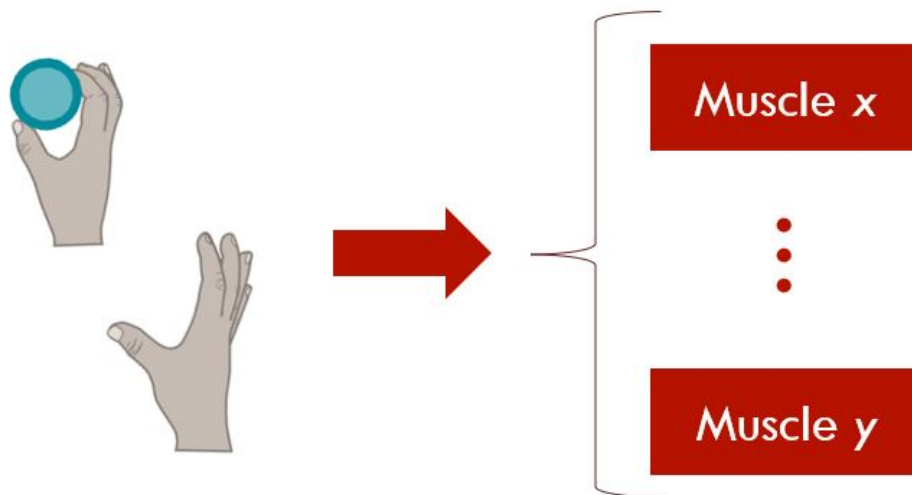


Figure 4.13: Labels creation - second step. [40].

4. At this point, signals are generated to obtain the different motion dynamics. In this step, account is taken of the fact that in some cases the signals cannot all be sent at the same time. In the case described above, where the movement is divided into two phases, the stimulation signals corresponding to the abduction muscles (and possibly the torsion muscles of the wrist) will have to be sent earlier than the signals stimulating the adduction muscles. Each signal is defined by its stimulation parameters.

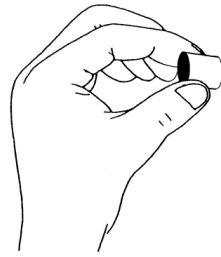


Figure 4.14: Grasping type example for small objects.

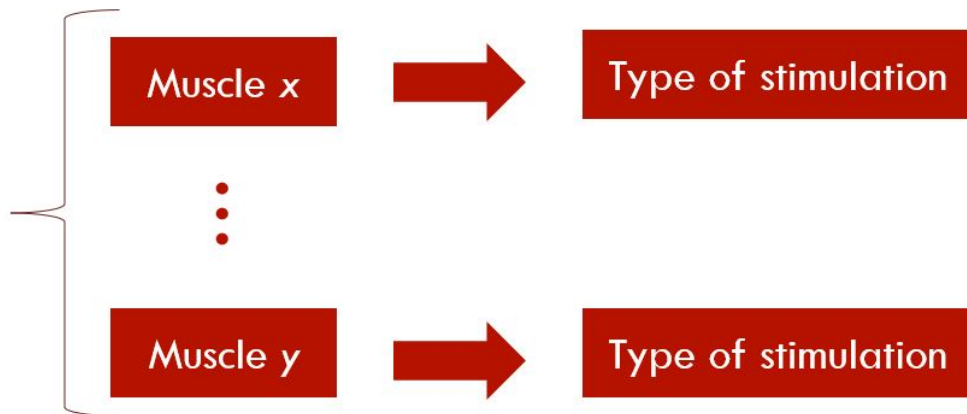


Figure 4.15: Labels creation - thrid step.

5. The last step is necessary to facilitate the work of the decoder. To avoid having N parameters for C channels, which would lead to NxC outputs from the decoder, the choice was made to encode a set of parameters with an integer. Each possible parameter set therefore corresponds to an integer number. This makes it possible to have as output of the decoder a vector of M integer values, where M is the number of muscles of which the chosen set is composed (Fig.4.16).

4.4 Brain signals decoder

Once the new labels had been constructed, a new database was in fact defined. The signals to be decoded are still signals processed by iEEG records. However, the outputs are no longer objects encoded by two-digit numbers, but electrical parameters to be sent to 11 muscles on 11 independent channels.

Four decoders were examined to compare their performance and identify the one with the most potential for this type of application. At the suggestion of the

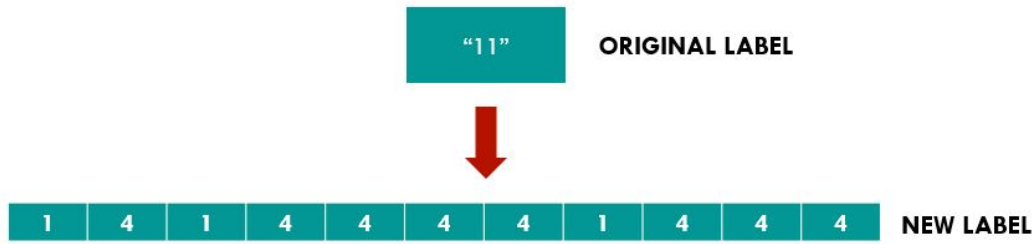


Figure 4.16: Example of original label and corresponding new label.

research group in which this thesis was carried out, the selection was made from among the decoders developed previously with the objective of object classification and subsequent implementation of the mechanical arm, in order to observe their capabilities in this new application, namely muscle stimulation through the FES technique. The decoders selected for comparison were therefore those based on DNN, RNN, LSTM and Ensemble Neural Network constructed by combining CNN and LSTM, respectively.

As the available decoders were developed with the objective of classification, first of all, a readjustment of the neural networks to a regression was necessary, as the values to be predicted in the case of this work are electrical parameter sets. In a first step, the decoders were tested using the optimised parameters using the old labels, i.e. the coded objects. In a second step, the optimisation of the parameters was re-performed using the new dataset, after which the decoders were tested again. Since in the previous work, the most successful neural network was the Ensemble, it was expected that it would also perform better than the others in this case. The steps of the work are explained in detail below.

4.4.1 Decoders selection

Previous work consisted of decoding the same signals for the implementation of the mechanical arm. The labels of the neural networks were the grasped objects encoded by two-digit numbers. The decoders tested were based on the following types of neural networks: Dense Neural Network (DNN), Convolutional Neural Network (CNN), Gated Recurrent Unit (GRU) Neural Network, Simple Recurrent Neural Network (RNN), Long Short-Term Memory (LSTM) Neural Network, Ensemble (CNN+LSTM). Ensemble NN was the one that performed best in previous work, so the expectation was that it would perform better than all of them in this case as well. Of these, only DNN, RNN, LSTM and Ensemble neural networks were taken into account.

- The Dense Neural Network is one of the most famous neural networks and is inspired by the way the human brain processes information. This type of architecture is characterised by the fact that the layers are full-connected (Fig.4.17). This means that each neuron receives as input the output of all the neurons that make up the layer. The neurons optimise themselves through the learning process. The dense layer is capable of matrix multiplication, where the elements in the matrix are parameters that are updated through the process of backpropagation [41].

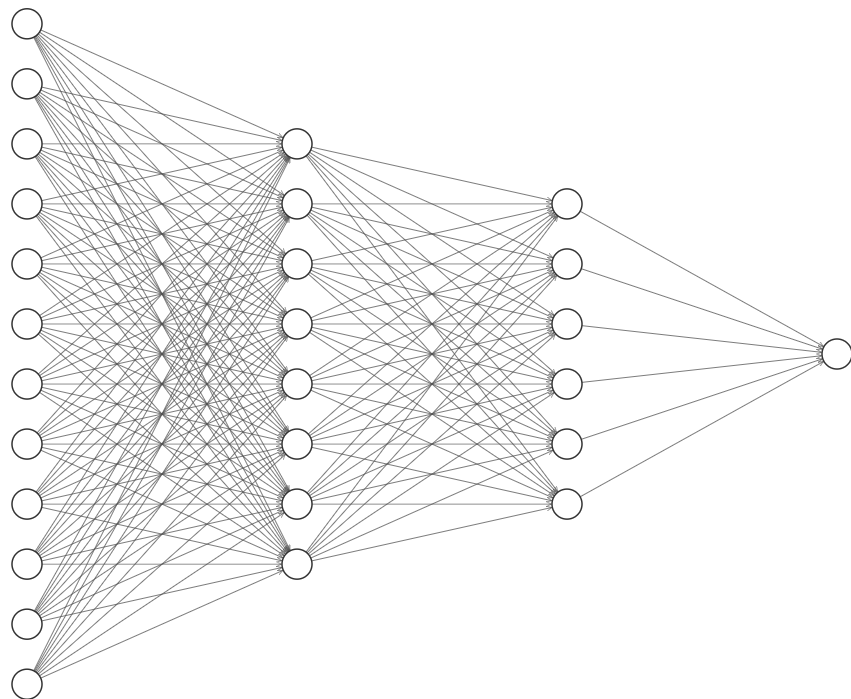


Figure 4.17: Dense Neural Networks.

- The Recurrent Neural Network is a type of neural network in which the output of a node can influence the input of the same node. Thus, cycles can occur within the neural network (Fig.4.18). RNNs are characterised by the fact that nodes of the same layer share parameters and the way to update parameters is a particular type of back propagation, which is back propagation through time (BPTT). This type of network is used when there are time series to be predicted, or more generally when dealing with temporal problems. RNNs are massively implemented for speech recognition and language translation.

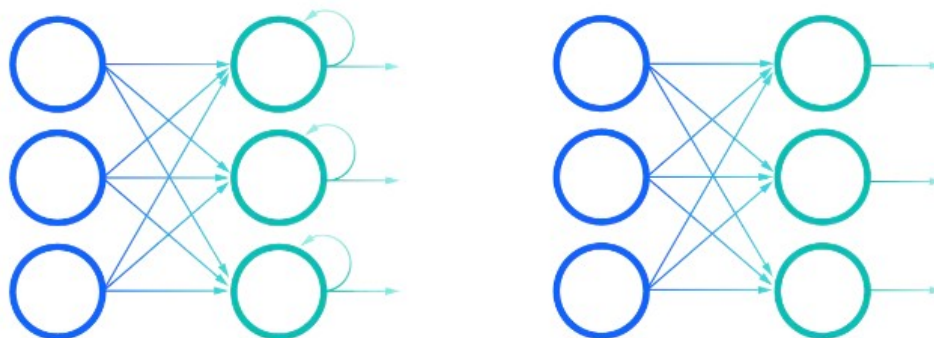


Figure 4.18: Recurrent Neural Network vs Feed Forward Neural Network [42].

- Long short-term memory (LSTM) neural network is a type of RNN that is more robust than a simple RNN with respect to the vanishing problem, as it handles long term dependencies by understanding when some learned information may be forgotten [43]. LSTMs are constructed in cells (Fig.4.19), in which the processes of information updating or elimination take place. These cells take as input two elements: cell state and hidden state. There are several gates in the cell: sigmoid gates are the gates through which the decision is made whether to add information or delete it. The sigmoid gates are present in two steps: in the first step they decide whether to delete part or all of the information from the previous unit; the second step is to take the new input and decide whether or not to keep the information and decide whether or not to update the new state. In the second step there is another operation obtained by a tanh gate, which gives the weight to the values that pass [44].
- Finally, the Ensemble Neural Network, created by combining CNN and LSTM, has the characteristic of separating spatial features from temporal features. The convolutional layer reduces the channel size and extracts the spatial features, while the LSTM layer handles the temporal dependencies.

4.4.2 Adaptation to new outputs

The neural networks with which the decoders selected from the previous work were constructed are classification neural networks. The outputs consisting of the number codes of the objects were encoded with the one-hot encoding.

With the new outputs, the problem becomes multi-class multi-label, since there are several parameter sets and at the same time, for each output there are 11

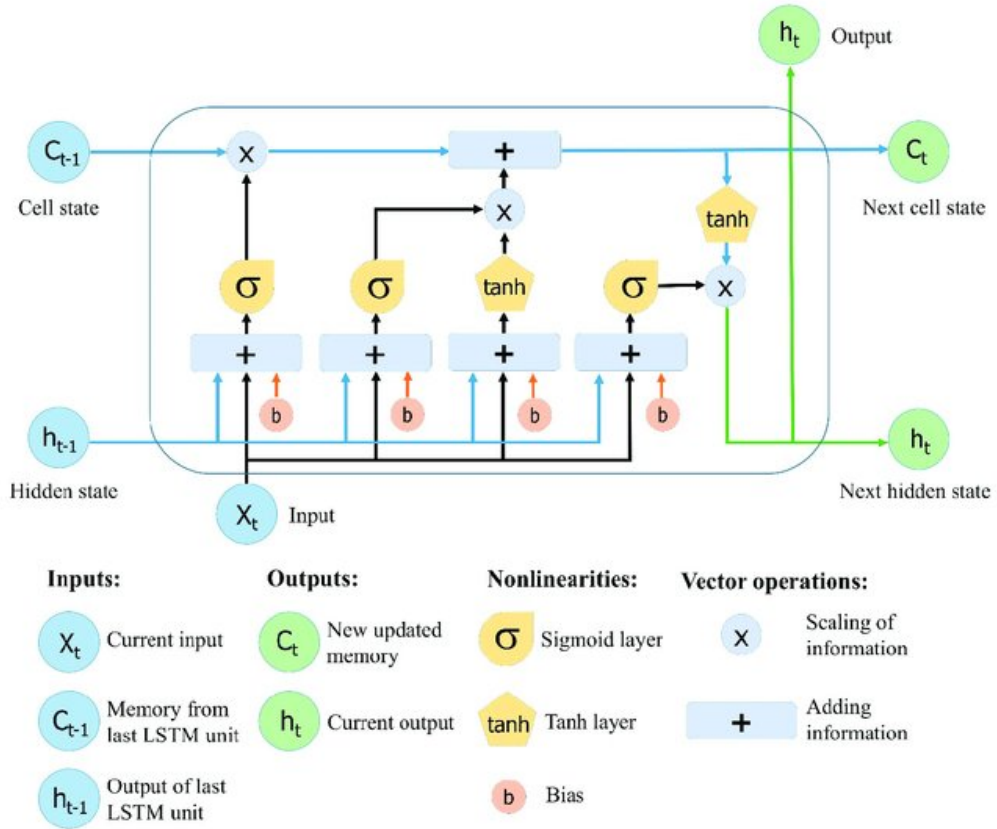


Figure 4.19: LSTM Neural Network structure [44].

parameter sets. The one-hot encoding approach can theoretically be extended to the new outputs by using multi-hot encoding. However, multi-hot coding leads to the identification of 7 configurations as outputs, transforming the objective of attributing one parameter set to each muscle for each trial considered into the attribution of one parameter configuration for each trial. Since the intention in this project is to treat each muscle individually, it was decided not to use the multi-hot approach.

At this point, the chosen solution was to treat the problem as a multi-label regression problem. The values output by the neural network are therefore not integer values, but float numbers that do not correspond to any of the constructed parameter sets. To transform these float numbers into integers, we chose to round them to the nearest integer value and consider the rounded value as the identifier of the parameter set to be assigned to each muscle.

Since the problem cannot be one hot encoded, but you have 11 labels per output with 6 possible values, further modifications had to be made to the neural networks, such as the activation function in the output layer. First, since each of the eleven

labels per output must be treated independently, the activation function 'sigmoid' was used [45] in first place:

$$\sigma(z) = \frac{1}{1 + e^{-z}} \quad (4.1)$$

However, since this type of function is suitable for binary classification, and multi-hot encoding was not used in this project, the chosen activation function was linear, since the problem was eventually treated as a regression problem.

In addition, since we in fact consider the problem a regression, the metric to be used within the optimisation is the mean squared error. Accuracy is only calculated later, after all outputs have been transformed into integers. The original labels are then compared with the outputs of the neural network and compute the accuracy for each stimulated muscle and finally the mean accuracy over all muscles.

4.4.3 Hyperparameters optimization

The starting neural networks are characterised by hyperparameters chosen using TPE (Tree Parzen Estimator). Before making the same choice for the optimisation of the hyper-parameters with the new dataset, a literature search was carried out of the different methods of optimising hyper-parameters and establishing which is preferred in the state of the art. At this stage, the major contribution was made by a 2020 review, "Hyper-parameter optimisation: A review of algorithms and applications" [46].

- The grid search is a very simple method based on the combined use of a number of parameters in a range decided by the user. This method is therefore tied to the experience of the user, who defines the ranges of values to search from based on prior knowledge.
- Random search is a technique similar to grid search, but which in general seems to perform better in the case of non-uniformly distributed hyperparameters. It is a search for hyperparameters within certain distributions. The search continues until the defined condition (e.g. accuracy) is fulfilled.
- Bayesian optimisers are more efficient than the previous two, as the optimisation process is guided by experience from previous trials. However, they are more computationally demanding than grid search and random search.
- Tree Parzen Estimators are derived from Bayesian Optimisers, but in deep learning they are more widely used than the originals as they are more flexible on data types. This technique selects subsequent hyperparameters based on the expected improvement. In this algorithm, once a hyper-parameter is found

that performs well, it continues to search for a value in the vicinity of that parameter.

Since, compared to the time of the precedent work, there do not seem to have been any noticeable improvements in the development of optimisation techniques and the library available in python 'hyperopt' makes the TPE method easily usable, it was decided to retain it in this work as well. However, the number of conformations to be tested was reduced, as the output data is more complex than in the old dataset and the search time for optimal hyperparameters increases considerably. For each neural network, the number of configurations tested was 100.

The hyperparameters optimized by TPE are the number of units, the batch size, the number of epochs and the dropout. The dropout, in particular, is an hyperparameter introduced for the regularization, so to avoid overfitting and it consists in temporally deleting units from the neural network.

4.4.4 Training, validation and test

The dataset was divided into training, validation and test. Specifically, 70% was used as the training set, 15% as the validation set and the remaining 15% as the test set. In addition, K-fold cross validation was applied as re-sampling procedure since there is little data available. This method serves to ensure greater robustness of the algorithm. For the purpose of K-fold cross validation, only the training set and the validation set were considered. $K = 5$ was used, so 5 training sets and 5 validation sets were generated. The procedure is described below [47]:

1. Shuffle the dataset.
2. Split the dataset into $K = 5$ subsets.
3. One subset corresponds to the validation set.
4. The other four subsets together correspond to the training subset.
5. Fit the model on the training subset and evaluate it on the validation subset.
6. Save the evaluation score.
7. Switch the validation subset, repeat from 3 to 6, until all of the subsets were validation subset once.

This split was exploited both in hyperparameters optimization and in training, validating and testing data.

Chapter 5

Results

5.1 Muscle selection

Most of the devices used for FES are multichannel. Therefore, several muscles can be stimulated by sending the stimulation signals for each muscle through the corresponding channel. Each channel receives a set of stimulation parameters from the brain signal decoder. In particular, each output of the decoder corresponds to a channel. The structure of the decoder is described in detail in section 5.4. The fact that stimulators are multichannel does not mean, however, that they have an infinite number of channels available for stimulation. Taking into account that a channel corresponds to a muscle to be stimulated, a choice was made among the muscles described in section 4.1. In particular, the set of muscles chosen for the hypothesised grasping types contains 11 muscles.

Of the two forearm muscles (extensor digitorum communis and flexor digitorum superficialis), the flexor digitorum superficialis was chosen. The reason lies in the fact that, in the first phase of the grasping movement of the objects in the dataset, the flexion of the fingers plays a primary role compared to their extension. We therefore want to privilege this movement and delegate the action of extension to the smaller muscles residing in the hand. The flexion of the fingers ensures that the subject is able to hold the object. The release movement, in which all the muscles associated with extension would take over in a voluntary movement, would only be performed in this case through the absence of stimulation: once the stimulation signals to the muscles have stopped, the hand tends to resume its naturally relaxed conformation.

Of the three thenar muscles (flexor pollicis brevis, abductor pollicis brevis and opponens pollicis), only the opponens pollicis was chosen, whose action is to move the thumb away from the fingers. As explained in Methodology, this is one of the most important muscles of the thenar muscles and intervenes in the first phase of

grasping larger objects, in which it is necessary to slightly extend the thumb. The adductor pollicis is another muscle that controls the movement of the thumb but it is not part of the thenar group. This muscle has the function of thumb adduction, which is necessary in the grasping of all objects and was therefore selected.

All the interossei muscles were then selected: 4 dorsal and 3 palmar. This choice is due to the fact that, for smaller objects, the movement of only some of the fingers is necessary. Take for example the grasping of a small ball, where only the thumb, index and middle finger are involved. There is therefore a need for selectivity in stimulation when dealing with objects of various sizes. Again, there are muscles assigned to abduction (dorsal) and those assigned to adduction (palmar).

For the torsion of the wrist, since it is a movement composed of the action of several muscles, the ideal would be to create a specific and more complex stimulation in order to perform all the movements necessary for the torsion in sequence. However, in this first simulated approach, the group of muscles is considered as a single muscle capable of performing the entire twisting action using the same stimulation signals created for the other muscles. In the development of the software, each of the chosen muscles was assigned a numerical code, as can be seen in Tab.5.1.

Code	Muscle
10	Flexor digitorum superficialis
20	Opponens pollicis
30	Adductor pollicis
41	Interossei dorsal 1
42	Interossei dorsal 2
43	Interossei dorsal 3
44	Interossei dorsal 4
51	Interossei palmar 1
52	Interossei palmar 2
53	Interossei palmar 3
60	Wrist twist muscles group

Table 5.1: Chosen muscles and their codification for the software development.

5.2 FES signals

Following the study of FES signals and considerations already presented in section 4.2 in 4, it was decided to use the same waveform for the stimulation signal for all the muscles to be stimulated. As explained in the previous section, it is generally preferred to use balanced bipolar signals to ensure that there is no excess charge in the tissue, as would be the case using monophasic waveform signals. For these reasons, the choice falls on the symmetric bipolar waveform or the balanced asymmetric bipolar waveform.

In contrast, amplitude, duration and frequency are generally parameters that can vary. In particular, the combination of amplitude and duration defines the intensity of the stimulation, and therefore of the contraction.

For example, to stimulate larger muscles, such as the flexor digitorum superficialis muscle, a higher current or duration of stimulation is required than for interossei stimulation.

The values chosen for the stimulation parameters are therefore as follows:

- Pulse amplitude: 10 mA for small muscles and 20 mA for the flexor digitorum superficialis muscle, the only large one compared to the others.
- Pulse duration: 0.5 s for all muscles.
- Frequency: 30 Hz for all muscles.

In addition, since in some cases, as explained in section 4.3, the movement takes place in two phases, with stimulation of the abductor muscles before the adductor ones, the signals are characterised by a delay: typically, the adductor muscles is to be stimulated in the second phase, then the delay is at the beginning of the stimulation, while for the abductor muscles, the delay is at the end of the stimulation in the second phase, since we stop stimulating them when the fingers are extended. In Fig.?? the stimulation signals for small muscles with symmetrical biphasic waveform are shown. Tab.5.2 shows the stimulation parameters for all the signals considered in this work. The set number will be also the element in the vector which is the output of the neural network.

5.3 Dataset labels construction

Following the steps described in Sec.4.3, the groups of signals corresponding to the 11 chosen muscles were generated. Considering that different objects in the dataset may have the grasping conformation in common, the configurations were grouped together, resulting in 8 configurations in total. By configuration we mean the set of stimulated muscles and the stimulation parameters associated with them.

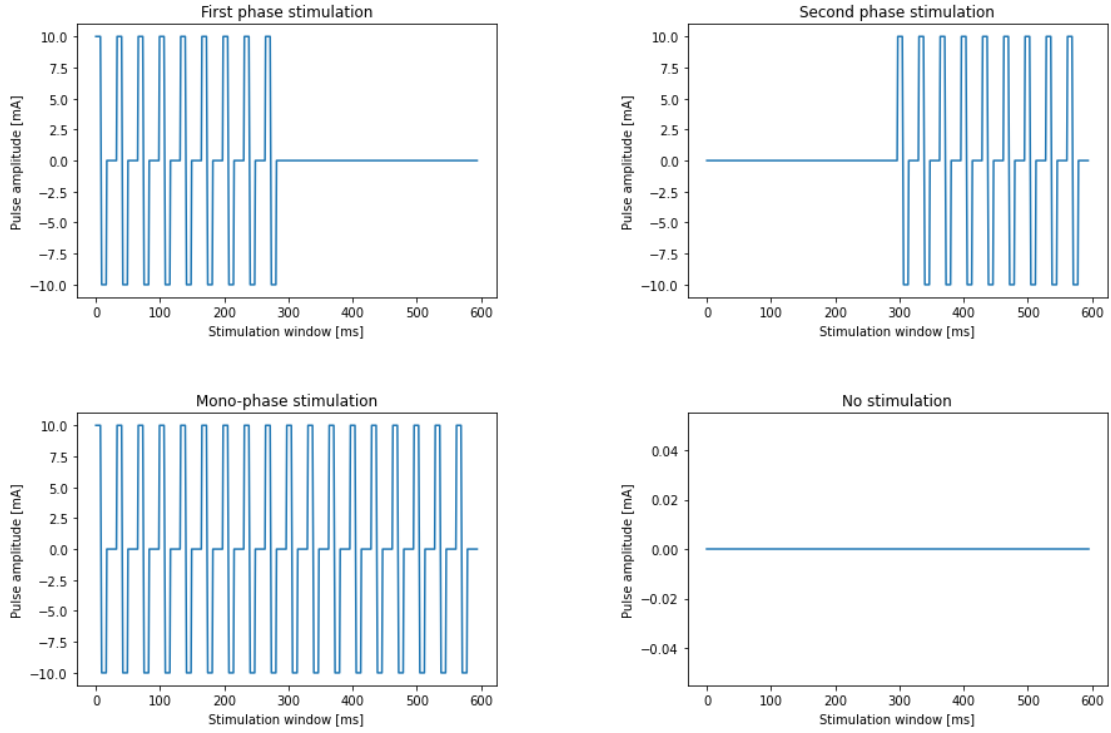


Figure 5.1: Stimulation signals.

Set	Pulse amplitude	Pulse duration	Frequency	Delay in	Delay out
1	10mA	0.5s	30Hz	No	No
2	10mA	0.5s	30Hz	Yes	No
3	10mA	0.5s	30Hz	No	Yes
4	0mA	0s	0Hz	No	No
5	20mA	0.5s	30Hz	Yes	No
6	20mA	0.5s	30Hz	No	Yes

Table 5.2: Set of parameters.

Each two-digit label was then replaced by a vector of 11 items, where each item can take a value between 1 and 6. Each item corresponds to a specific set of parameters. To understand the correspondence between each integer and the set of electrical parameters it identifies, observe Tab.5.2. Of the eight configurations constructed, only seven are actually used, while the eighth configuration is an

auxiliary configuration consisting of all $0mA$ signals, preliminary associated with tasks whose labels were not clear. Taking into account the encoding of the electrical parameter sets in Tab.5.2 and the condensing of the chosen muscles in Tab.5.1, all the generated configurations are presented in Tab.5.3. The configurations associated with the objects related are shown in Fig.5.2

Configuration	M10	M20	M30	M41	M42	M43	M44	M51	M52	M53	M60
C1	5	4	1	4	4	4	4	1	4	4	4
C2	6	3	2	3	3	3	3	2	2	2	4
C3	5	4	1	4	4	4	4	1	1	1	4
C4	5	4	1	4	4	4	4	1	1	4	4
C5	6	3	2	3	3	3	3	2	2	2	3
C6	6	4	2	4	4	4	4	2	4	4	3
C7	6	4	2	4	4	4	4	2	2	4	3
C8	4	4	4	4	4	4	4	4	4	4	4

Table 5.3: Muscle stimulation configurations.

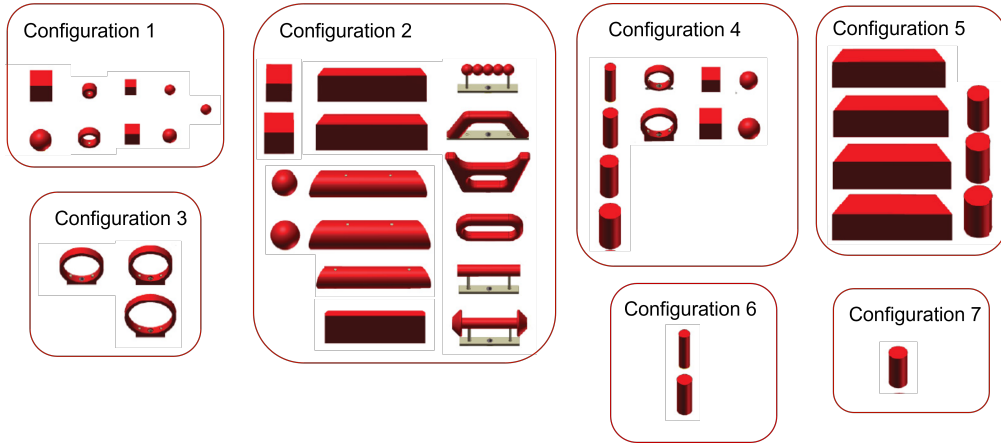


Figure 5.2: Configurations and corresponding objects.

Since the construction of the new labels, however, a problem has arisen. Since one configuration can correspond to several objects, the labels appear with a widely varying cardinality in the dataset (Tab.5.4), thus generating a polarity that can negatively affect the output of a neural network. Some configurations appear in significantly greater numbers than others. An approach must therefore be chosen to minimise these differences in the dataset, without decreasing the cardinality too much. Two approaches are considered:

- Find the lowest number of appearances among all m labels and use m trials for each type of label.
- Average the number of times each label appears. Reduce the number of tasks with labels that appear in the dataset more than the average to a number equal to the average.

The first approach was discarded in this case, as the lowest number of appearances corresponds to configuration 7, which appears only 12 times in the dataset. If one were to reduce all tasks per label to 12, one would have $12 * 7 = 84$ samples in the whole dataset, which is too few for a neural network. It was therefore preferred to use the second approach. Although the problem remains, the impact that the samples appearing several times now have on the entire dataset is less than before. The new cardinality of the labels is shown in Tab.5.4

Configuration	N of samples before filtration	N of samples after filtration
1	97	67
2	111	67
3	32	32
4	118	67
5	81	67
6	21	21
7	12	12

Table 5.4: Occurrences of labels in the original and in the filtered datasets.

5.4 Brain signals decoder

5.4.1 Hyperparameters optimization

The neural networks were customised for the new dataset and the new problem type. Certain characteristics were chosen with the new problem under consideration in mind, namely regression instead of classification. These include the activation function of the output layer, the loss rate and the metric used during training. Other parameters were set using the TPE algorithm, as explained in 4.4.3. This group includes the number of units, the batch size, the number of epochs and the fractional dropout. The searching space for hyperparameters is made by discrete numbers, but usually when TPE is used, the neighbourhood where to look for better

values is made by a continuous space. In this case, then, when the algorithm finds a good hyperparameter, it will use the same one for the next run. The searching spaces used for the neural networks are the following:

- DNN space:
'num neurons': 32, 640, 32,
'frac dropout': 0., 0.5, 0.05,
'n epochs': 5, 50, 5,
'batch size': 2, 26, 2.

- RNN space:
'num units': 16, 256, 16,
'frac dropout': 0., 0.5, 0.05,
'n epochs': 5, 50, 5,
'batch size': 2, 26, 2.

- LSTM space:
'num units': 16, 256, 16,
'frac dropout': 0., 0.5, 0.05,
'n epochs': 5, 50, 5,
'batch size': 2, 26, 2.

- Ensemble space:
'n filters': 4, 64, 4,
'size': 16, channels/2, 16,
'activation': ['relu', 'elu'],
'frac dropout': 0., 0.5, 0.05,
'pooling layer': ['max', 'avg']),
'n units': 16, 256, 16,
'n epochs': 5, 50, 5,
'batch size': 2, 26, 2.

Optimisation was carried out taking into account the average loss of each configuration and trying to minimize it. In Fig.5.3, 5.4, 5.5, 5.6 the loss evolution during the optimisation for all networks is shown. For the DNN, RNN and LSTM neural networks, the loss did not vary much during the validation of the different configurations. This may be due to the fact that after only a few configurations, good values were found and the hyperparameters' space was not explored extensively, but remained around the values that performed well in the first iterations.

The same cannot be said of the Ensemble neural network, whose loss changes considerably during the validation of the 100 configurations. This is probably due to the difficulty of the TPE algorithm in finding 'good' values in whose neighbourhood it searches for optimal values. It is natural to think that in this case the space was more explored than in the other networks. In addition, one must consider that the space of the hyperparameters in this case also has more dimensions than the spaces of the other neural networks, as more hyperparameters have been subjected to optimisation. This certainly creates more difficulties for the algorithm and, in order to reach a steady state in the loss evolution, a much larger number of iterations should be used.

For each type of neural network used, the found hyperparameters can be observed in Tab5.5. For the Ensemble neural network, the optimised hyperparameters were more than for the other networks. In particular, the number of filters was set to 32, the pooling layer to 'max', activation function to 'elu'.

Network	Number of units	Batch size	Number of epochs	Fractional dropout
DNN	128	2	50	0.05
Simple RNN	176	2	45	0.2
LSTM	160	2	45	0.4
Ensemble	240	2	30	0.25

Table 5.5: Optimum hyperparameters.

5.4.2 Training, validation and test

Once the parameters optimising the performance of the neural networks had been found, they were trailed using the K-cross validation approach to obtain greater robustness, were then validated on the validation sets of the K=5 repetitions and finally tested on the test set. In Fig.5.7, the accuracy plots for training, validation and test sets for all muscles were collected. In Fig.?? the accuracy graph corresponding to the training set can almost be intercepted, as it is almost always close to 100% for both DNN and RNN. In contrast, validation and test sets show much lower accuracy. This suggests that we are dealing with the phenomenon of overfitting. These two networks, with the hyperparameters optimised using the TPE algorithm, therefore overfitting. If we look again at Tab.5.5, we can see that the dropout fraction values chosen for these networks is very low. Usually, to avoid phenomena such as overfitting, the dropout fraction must have values between 0.5 and 0.8. Therefore, the accuracies for the DNN and RNN neural networks were re-evaluated with the dropout fraction first being 0.5 and then 0.8. The same was also done for the other two networks, for comparability. The results can be seen in

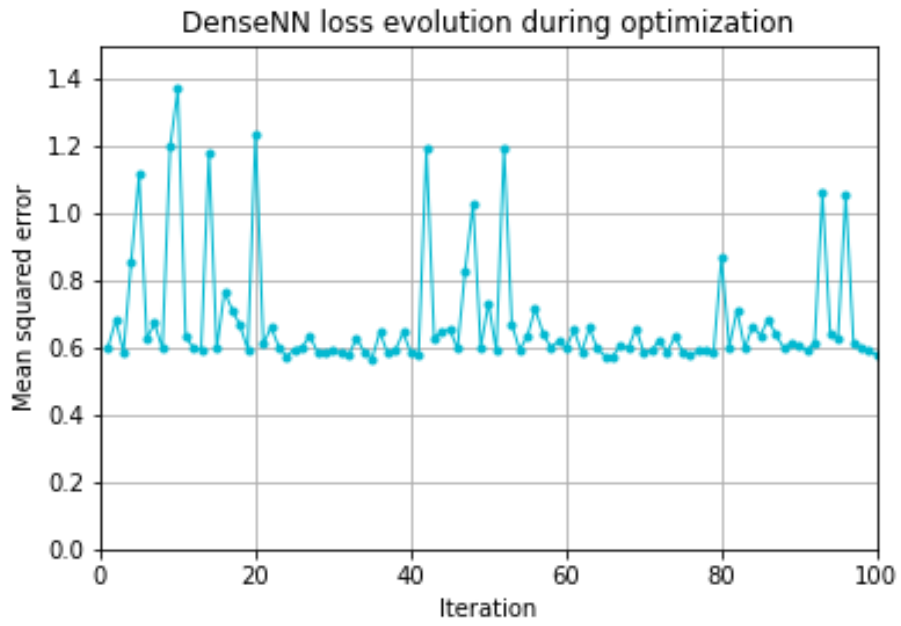


Figure 5.3: Dense Neural Network loss evolution.

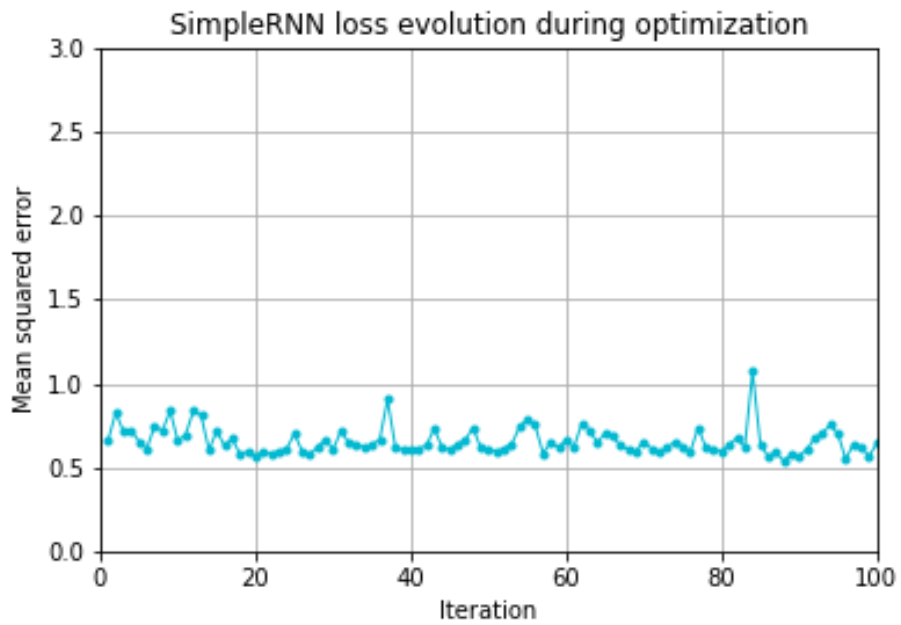


Figure 5.4: Simple Recurrent Neural Network loss evolution.

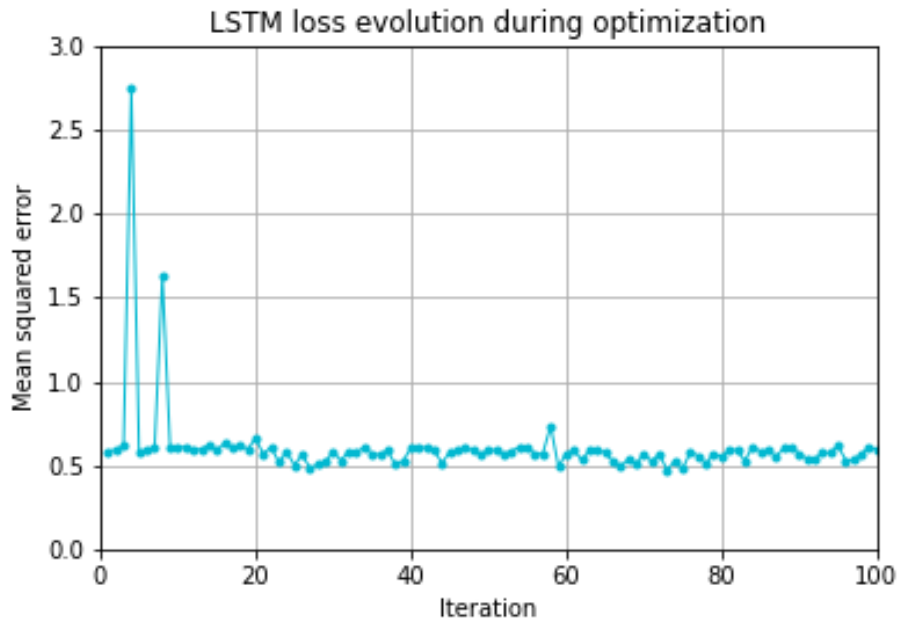


Figure 5.5: LSTM Neural Network loss evolution.

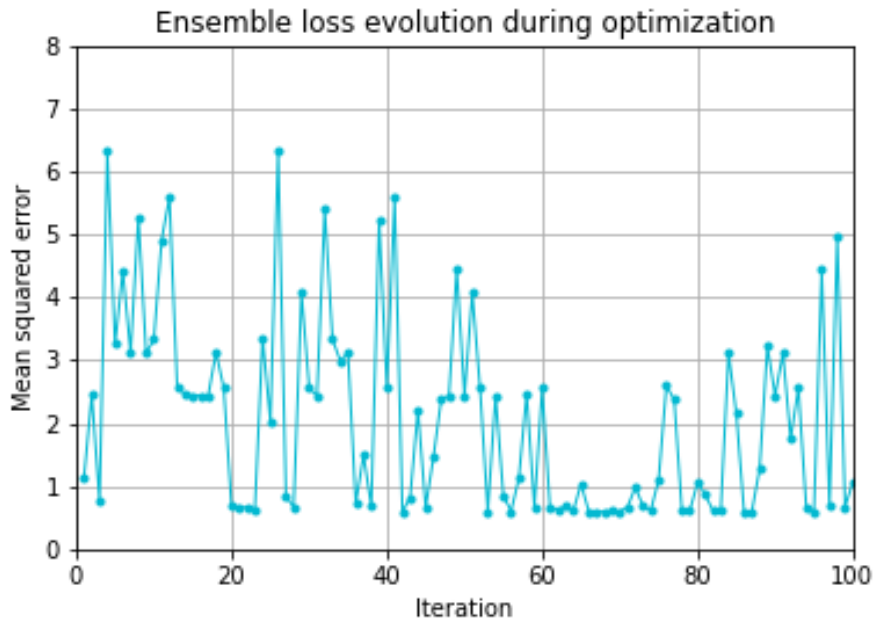


Figure 5.6: Ensemble Neural Network loss evolution.

Tab.5.6. The accuracy values in this table were calculated by averaging over the accuracy of all muscles. Focusing on DNN, as the dropout fraction increases, the accuracy on the training set decreases, while the accuracy values on validation and test sets are rather stable. The substantial difference between accuracy on the training set and the other two sets remains intact. Therefore, even having introduced a regulating effect in this network, overfitting is not entirely avoidable. As far as the Simple RNN network is concerned, the same mechanism can be observed as just explained. What is different is only an increase in the accuracy on the validation set, but the difference between the accuracy on the training set and the accuracy on the validation and test set is even greater than in the case of the DNN. Again, the overfitting phenomenon was not eliminated even when the dropout fraction was increased to a very high value.

In the case of these first two neural networks, overfitting led to very good predictive ability on the training data and very low performance on the validation and test set. The average accuracy values are in fact around 50 per cent for these sets, which is equivalent to a random choice of parameters with which to stimulate the various muscles. Undoubtedly a not inconsiderable weight in the lowering of the average accuracy is due to the network's inability to assign the correct set of stimulation parameters to the "53" muscle in particular, hence the lowest accuracy is found in both DNN and RNN.

On the other hand, looking at Fig.5.8, one notices first of all that there is

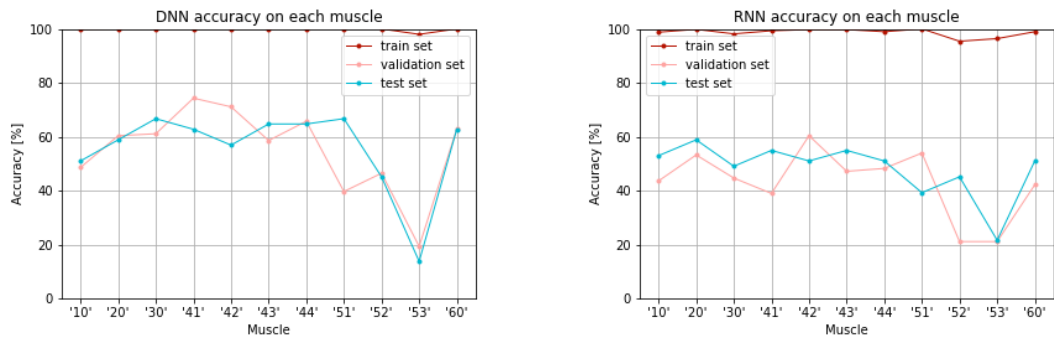


Figure 5.7: Accuracy with optimized hyperparameters for DNN and RNN.

no overfitting in the training of the Ensemble neural network. However, the performance is very low and, in particular, the problem on muscle '53' is maximised here, resulting in an accuracy of 0 for this muscle.

A possible explanation for the network's difficulty in assigning the right set of stimulation parameters to this muscle could be the fact that it is part of the interosseus palmar group and usually the three muscles are always stimulated

together. However, there are trials corresponding to small objects and in these cases, this muscle should not be stimulated. However, the three neural networks are not able to differentiate these cases. On the contrary, as Fig.5.9 suggests, the LSTM neural network not only does not exhibit the phenomenon of overfitting, but also performs much better than the other neural networks. Although the problem on muscle '53' is still present, it has less weight on the average accuracy of the network, which is about 63% on the validation set and 67% on the test set. This is still not a very good result, but it is reasonable and reliable in proportion to the size of the dataset and the fact that the labels were artificially generated.

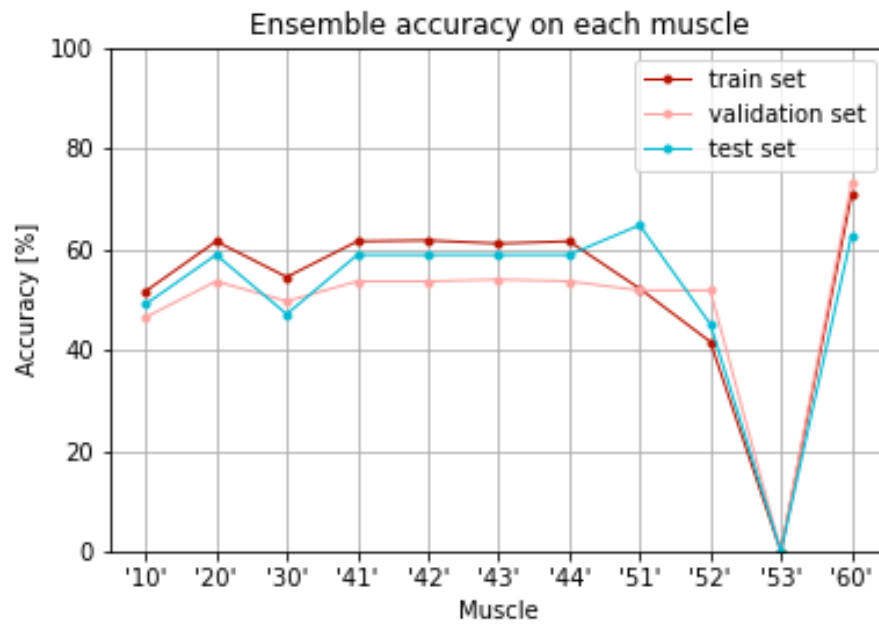


Figure 5.8: Ensemble accuracy.

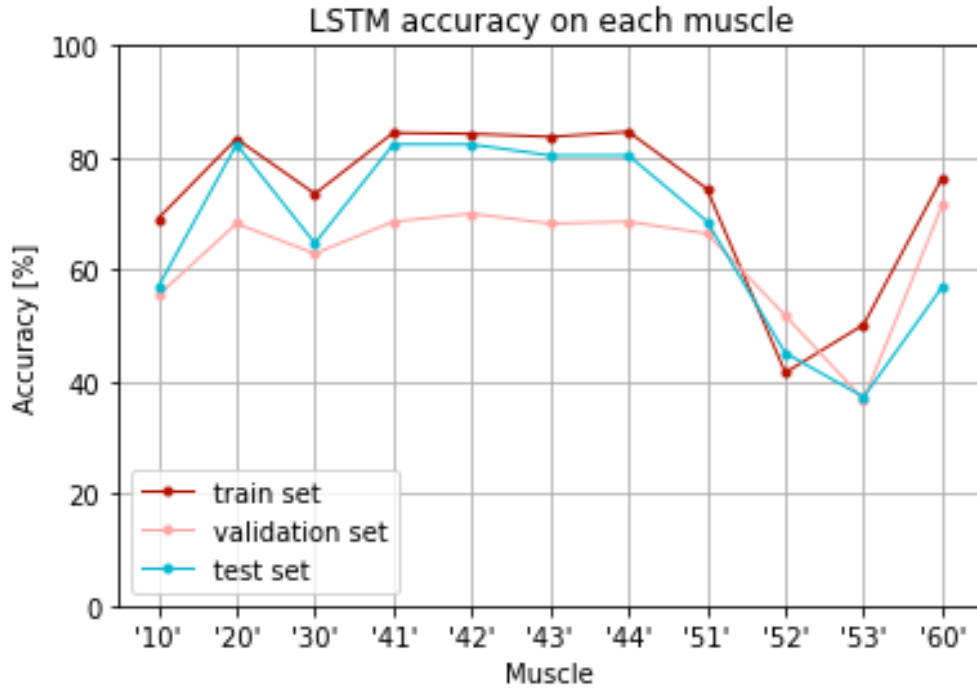


Figure 5.9: LSTM accuracy.

	Dataset	Acc. opt. df	Acc. df = 0.5	Acc. df = 0.8
DNN	Training	99.95%	93.61%	81.12%
	Validation	53.21%	53.54%	51.46%
	Test	57.22%	55.44%	54.19%
RNN	Training	98.65%	94.70%	86.61%
	Validation	43.12%	47.40%	49.22%
	Test	48.13%	44.03%	42.96%
LSTM	Training	73.23%	73.03%	70.76%
	Validation	62.57%	63.47%	60.84%
	Test	67.02%	67.91%	62.92%
Ensemble	Training	52.53%	44.85%	48.69%
	Validation	49.19%	46.59%	47.73%
	Test	51.16%	42.96%	49.73%

Table 5.6: Accuracy for different values of dropout fraction.

Chapter 6

Conclusions

In this work, the decoding of intra-cranial signals for decoding grasping information was attempted. The final goal was to predict the electrical parameters to implement the FES technique. After simulating the muscles and the electrical parameters with which to stimulate them, four different decoders were tested, of which the one based on LSTM appears to be the most promising, with an accuracy of more than 60% on the test set.

However, this is a limited result, since the application under test is very sensitive. These are in fact neuroprostheses, which must be safe in the first place and must guarantee good function. The relative poor performance in this case is due to several factors. Firstly, the fact that we had to remove many trials from the already limited dataset contributed negatively to the network's learning capacity. It is indeed crucial for a neural network to have a lot of data available in order to be able to learn properly how to replicate choices in the case of prediction. Having little data available, despite the regularisation work, inevitably leads some networks to overfitting, and in general to poor performance on new data.

Secondly, the labels were created entirely artificially. They therefore do not have the reliability of real data and therefore no clear judgement can be made on the quality of the results.

6.1 Future work

In order to develop the work in a more robust manner using artificial intelligence, the dataset must be greatly expanded so as to have as many samples as possible on which the network can learn.

In addition, the way to make the results clear and reliable is to perform the experiment simultaneously with the recording of electromyographic (EMG) signals, so that the muscles involved in each action during the experiment can be more

clear.

As far as FES signals are concerned, their characteristic is that they cannot have global parameters, i.e. that they work for all individuals indiscriminately. In order to create the different configurations with the various parameters, it is necessary to try out the stimulation device on the person in situ. This serves to select the values for the parameters that definitely work for the person in exam.

Bibliography

- [1] Thomas J Oxley et al. «Motor neuroprosthesis implanted with neurointerventional surgery improves capacity for activities of daily living tasks in severe paralysis: first in-human experience». In: *Journal of NeuroInterventional Surgery* 13.2 (2021), pp. 102–108. ISSN: 1759-8478. DOI: 10.1136/neurintsurg-2020-016862 (cit. on p. 1).
- [2] URL: <https://www.who.int/> (cit. on p. 1).
- [3] Cody L McDonald, Sarah Westcott-McCoy, Marcia R Weaver, Juanita Haagsma, and Deborah Kartin. «Global prevalence of traumatic non-fatal limb amputation». In: *Prosthetics and orthotics international* (2021) (cit. on p. 1).
- [4] Sheital Bavishi, Joseph Rosenthal, and Marcia Bockbrader. «Chapter 17 - Neuroprosthetics». In: *Rehabilitation After Traumatic Brain Injury*. Ed. by Blessen C. Eapen and David X. Cifu. Elsevier, 2019, pp. 241–253. ISBN: 978-0-323-54456-6. DOI: <https://doi.org/10.1016/B978-0-323-54456-6.00017-7> (cit. on p. 1).
- [5] Kevin Warwick. «Neuroengineering and neuroprosthetics». In: *Brain and neuroscience advances* 2 (2018), p. 2398212818817499 (cit. on p. 1).
- [6] URL: <https://www.neuraviper.eu/> (cit. on p. 1).
- [7] URL: <http://www.moregrasp.eu/project/Project>) (cit. on p. 1).
- [8] URL: <https://cordis.europa.eu/project/id/864729> (cit. on p. 1).
- [9] URL: <https://www.b-cratos.eu/> (cit. on p. 1).
- [10] Stefan Schaffelhofer, Andres Agudelo-Toro, and Hansjörg Scherberger. «Decoding a wide range of hand configurations from macaque motor, premotor, and parietal cortices». In: *Journal of Neuroscience* 35.3 (2015), pp. 1068–1081 (cit. on pp. 2, 10–12, 15).
- [11] Federico Fabiani. «Brain-machine interface for bionic prosthetic arm actuation». In: (2021) (cit. on pp. 2, 11).

- [12] Andrea Biasiucci, Benedetta Franceschiello, and Micah M Murray. «Electroencephalography». In: *Current Biology* 29.3 (2019), R80–R85 (cit. on p. 4).
- [13] Miaomiao Zhuang, Qingheng Wu, Feng Wan, and Yong Hu. «State-of-the-art non-invasive brain–computer interface for neural rehabilitation: A review». In: *Journal of Neurorestoratology* 8.1 (2020), pp. 12–25. ISSN: 2324-2426. DOI: <https://doi.org/10.26599/JNR.2020.9040001> (cit. on p. 4).
- [14] Borís Burle, Laure Spieser, Clémence Roger, Laurence Casini, Thierry Hasbroucq, and Franck Vidal. «Spatial and temporal resolutions of EEG: Is it really black and white? A scalp current density view». In: *International Journal of Psychophysiology* 97.3 (2015). On the benefits of using surface Laplacian (current source density) methodology in electrophysiology, pp. 210–220. ISSN: 0167-8760. DOI: <https://doi.org/10.1016/j.ijpsycho.2015.05.004> (cit. on p. 4).
- [15] Guido Pagana. «Lesson IV Neuroimaging». In: 2020 (cit. on p. 5).
- [16] Edson Amaro and Gareth J. Barker. «Study design in fMRI: Basic principles». In: *Brain and Cognition* 60.3 (2006), pp. 220–232. ISSN: 0278-2626. DOI: <https://doi.org/10.1016/j.bandc.2005.11.009> (cit. on p. 5).
- [17] Valentina Agostini. «Neuroengineering course». In: 2020 (cit. on pp. 5, 6).
- [18] Josef Parvizi and Sabine Kastner. «Promises and limitations of human intracranial electroencephalography». In: *Nature Neuroscience* 21 (Mar. 2018). DOI: 10.1038/s41593-018-0108-2 (cit. on p. 6).
- [19] Dilson E. Rassier. «Sarcomere mechanics in striated muscles: from molecules to sarcomeres to cells». In: *American Journal of Physiology-Cell Physiology* 313.2 (2017). PMID: 28539306, pp. C134–C145. DOI: 10.1152/ajpcell.00050.2017. URL: <https://doi.org/10.1152/ajpcell.00050.2017> (cit. on p. 7).
- [20] Reza Abiri, Soheil Borhani, Eric W Sellers, Yang Jiang, and Xiaopeng Zhao. «A comprehensive review of EEG-based brain-computer interface paradigms». In: *Journal of neural engineering* 16.1 (Feb. 2019), p. 011001. ISSN: 1741-2560. DOI: 10.1088/1741-2552/aaf12e (cit. on p. 7).
- [21] Matija Milosevic, Cesar Marquez-Chin, Kei Masani, Masayuki Hirata, Taishin Nomura, Milos R. Popovic, and Kimitaka Nakazawa. «Why brain-controlled neuroprosthetics matter: mechanisms underlying electrical stimulation of muscles and nerves in rehabilitation». In: *BioMedical Engineering OnLine* 19 (2020) (cit. on pp. 7, 19–22).

- [22] G. M. Odegard, T. L. Haut Donahue, D. A. Morrow, and K. R. Kaufman. «Constitutive Modeling of Skeletal Muscle Tissue With an Explicit Strain-Energy Function». In: *Journal of Biomechanical Engineering* 130.6 (Oct. 2008). 061017. ISSN: 0148-0731. DOI: 10.1115/1.3002766 (cit. on p. 7).
- [23] Francesco Lullo, Coccia Armando, Anna Saltalamacchia, Cesarelli Mario, Bernardo Lanzillo, and D’Addio Giovanni. «Functional Electrical Stimulation for Upper Limbs Flexion-Extension and Prehension Movements in Rehabilitation». In: *Journal of Advanced Health Care* (Sept. 2020). DOI: 10.36017/JAHC2009-001 (cit. on pp. 8, 21).
- [24] Jayme S. Knutson, Nathaniel S. Makowski, Kevin L. Kilgore, and John Chae. «43 - Neuromuscular Electrical Stimulation Applications». In: *Atlas of Orthoses and Assistive Devices (Fifth Edition)*. Ed. by Joseph B. Webster and Douglas P. Murphy. Fifth Edition. Philadelphia: Elsevier, 2019, 432–439.e3. DOI: <https://doi.org/10.1016/B978-0-323-48323-0.00043-3> (cit. on p. 8).
- [25] Cesar Marquez-Chin and Milos R Popovic. «Functional electrical stimulation therapy for restoration of motor function after spinal cord injury and stroke: a review». In: *Biomedical engineering online* 19.1 (2020), pp. 1–25 (cit. on pp. 8, 9, 20, 21).
- [26] Thomas Brochier, Rachel L Spinks, Maria A Umilta, and Roger N Lemon. «Patterns of muscle activity underlying object-specific grasp by the macaque monkey». In: *Journal of neurophysiology* 92.3 (2004), pp. 1770–1782 (cit. on p. 15).
- [27] URL: <https://teachmeanatomy.info/> (cit. on pp. 16, 18, 19).
- [28] URL: <https://anatomifysiologi.se/anatomi/muskler/m-flexor-digitorum-superficialis/> (cit. on p. 16).
- [29] URL: https://en.wikipedia.org/wiki/Extensor_digitorum_muscle (cit. on p. 17).
- [30] Kwesi Dawson-Amoah and Matthew Varacallo. «Anatomy, Shoulder and Upper Limb, Hand Intrinsic Muscles». In: *StatPearls [Internet]*. StatPearls Publishing, 2021 (cit. on p. 16).
- [31] Edie Benedito Caetano, João José Sabongi, Lucas Augusto Ayres Ribas, and Edson Vimcius Milanello. «Accessory muscle of the flexor digitorum superficialis and its clinical implications». In: *Revista Brasileira de Ortopedia* 52 (2017), pp. 731–734 (cit. on p. 17).
- [32] Lauren Okafor and Matthew Varacallo. «Anatomy, shoulder and upper limb, hand flexor digitorum superficialis muscle». In: (2019) (cit. on pp. 17, 18).

- [33] Brandon E Lung and Ryan M Siwec. «Anatomy, Shoulder and Upper Limb, Forearm Flexor Carpi Ulnaris Muscle». In: *StatPearls [Internet]*. StatPearls Publishing, 2022 (cit. on p. 18).
- [34] Tadi P Sawyer E Sajjad H. «Anatomy, Shoulder and Upper Limb, Forearm Extensor Carpi Ulnaris Muscle». In: *StatPearls [Internet]*. StatPearls Publishing, 2022 (cit. on p. 18).
- [35] Dillon C Benson, Kathleen H Miao, and Matthew Varacallo. «Anatomy, Shoulder and Upper Limb, Hand Flexor Pollicis Longus Muscle». In: *StatPearls [Internet]*. StatPearls Publishing, 2021 (cit. on p. 18).
- [36] Keith L Moore, Arthur F Dalley, and Anne MR Agur. *Clinically oriented anatomy*. Lippincott Williams & Wilkins, 2013 (cit. on p. 18).
- [37] Irfan A Khan and Matthew Varacallo. «Anatomy, shoulder and upper limb, hand extensor pollicis longus muscle». In: *StatPearls [Internet]*. StatPearls Publishing, 2022 (cit. on p. 18).
- [38] Jing-jing Wan, Zhen Qin, Peng-yuan Wang, Yang Sun, and Xia Liu. «Muscle fatigue: general understanding and treatment». In: *Experimental & molecular medicine* 49.10 (2017), e384–e384 (cit. on p. 21).
- [39] W.M. Grill and J.T. Mortimer. «The effect of stimulus pulse duration on selectivity of neural stimulation». In: *IEEE Transactions on Biomedical Engineering* 43.2 (1996), pp. 161–166. DOI: 10.1109/10.481985 (cit. on p. 22).
- [40] Mariusz P Furmanek, Luis F Schettino, Mathew Yarossi, Sofia Kirkman, Sergei V Adamovich, and Eugene Tunik. «Coordination of reach-to-grasp in physical and haptic-free virtual environments». In: *Journal of neuroengineering and rehabilitation* 16.1 (2019), pp. 1–14 (cit. on pp. 23, 24).
- [41] URL: <http://alexlenail.me/NN-SVG/index.html> (cit. on p. 27).
- [42] URL: <https://www.ibm.com/cloud/learn/recurrent-neural-networks> (cit. on p. 28).
- [43] Sepp Hochreiter and Jürgen Schmidhuber. «Long short-term memory». In: *Neural computation* 9.8 (1997), pp. 1735–1780 (cit. on p. 28).
- [44] Xuan-Hien Le, Hung Viet Ho, Giha Lee, and Sungho Jung. «Application of long short-term memory (LSTM) neural network for flood forecasting». In: *Water* 11.7 (2019), p. 1387 (cit. on pp. 28, 29).
- [45] Neha Gour and Pritee Khanna. «Multi-class multi-label ophthalmological disease detection using transfer learning based convolutional neural network». In: *Biomedical Signal Processing and Control* 66 (2021), p. 102329 (cit. on p. 30).

- [46] Tong Yu and Hong Zhu. «Hyper-parameter optimization: A review of algorithms and applications». In: *arXiv preprint arXiv:2003.05689* (2020) (cit. on p. 30).
- [47] URL: <https://machinelearningmastery.com/k-fold-cross-validation/> (cit. on p. 31).